energy&fuels

pubs.acs.org/EF Review

Advances and Challenges in the Molecular Characterization of Petroporphyrins

Amy M. McKenna,* Martha L. Chacón-Patiño, Germain Salvato Vallverdu, Brice Bouyssiere, Pierre Giusti, Carlos Afonso, Quan Shi, and Marianny Y. Combariza

Cite This: https://doi.org/10.1021/acs.energyfuels.1c02002 Read Online

ACCESS | Metrics & More | Article Recommendations

ABSTRACT: Petroporphyrins, geoporphyrins, or metalloporphyrins are the original petroleum biomarkers, identified by Alfred Treibs more than a century ago and the first molecular evidence for the biogenic origins of petroleum. Since discovery, analytical strategies have been developed to identify porphyrins in petroleum and its fractions. This review focuses on the advances enabled by ultrahigh resolving power Fourier transform ion cyclotron resonance mass spectrometry in tribute to Professor Alan G. Marshall.

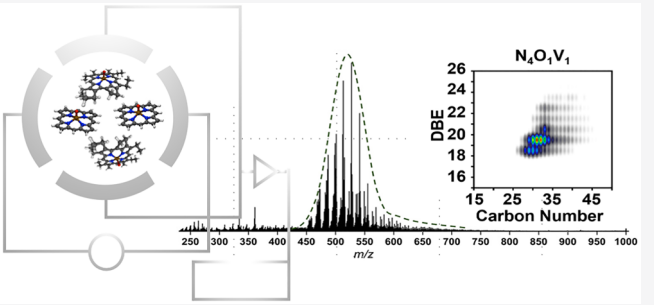

INTRODUCTION

Petroporphyrins, geoporphyrins, or metalloporphyrins together with other biomarker molecules elucidate processes and geologic conditions that dictate the molecular structure and composition of crude oil compounds.[1−5] Nickel, copper, vanadium, iron, and manganese porphyrins are tetrapyrrole-based metal complexes derived from chlorophylls and biologically active light- and oxygen-capturing molecules and are commonly found in fossil fuels (e.g., crude oils, bitumen, and oil sands), with nickel and vanadyl porphyrins commonly referred to as petroporphyrins.[6] Since the discovery of petroporphyrins by Alfred Treibs in the early 1930s, which provided the first molecular evidence for the biogenic origins of petroleum, many analytical techniques have been applied to characterize petroporphyrins (Treibs hypothesis).[1,4,5,7−11] Petroporphyrins, (e.g., nickel and vanadium) are geochemical marker molecules that contain information about fossil fuels genesis and are critical compounds with oil refining to determine a catalysts' performance.[12−16] The molecular structures of nickel and vanadyl petroporphyrins result from geochemical modifications to the original chlorophyll core (Figure 1, top row) caused by the mineral matrix, organic matter composition, and source rock conditions during early diagenesis and catagenesis (Figure 1),[16] including phytol loss, demetalation, aromatization by temperature and pressure, peripheral ring attachment, sulfur insertion, Ni/V derivatization, and finally transalkylation, commonly associated with thermal conversion and degradation during catagenesis.[17] Molecular transformations yield a range of structurally diverse porphyrin families that correspond to N_4VO, N_4VO_2, N_4VO_3, N_4VOS, and N_4Ni, depending upon the peripheral functional groups as shown in Figure 1 (bottom row).[13,16]

Very early, mass spectrometry provided invaluable insight into the molecular diversity of petroporphyrins compositions and structures.[1,4,5,18,19] In parallel, other analytical methods such as nuclear magnetic resonance (NMR) spectroscopy[19] and crystallography[20] afforded valuable insights on the structures of purified samples and, more recently, direct molecular imaging with atomic force microscopy molecular imaging.[21] A recent article introduces the phrase "metal-opetroleomics" and provides a comprehensive review on fractionation and characterization of petroleum asphaltenes to study metalloporphyrins.[22] Additional reviews on methods for studying petroleum porphyrins,[23] mass spectrometry on geoporphyrins,[24] petroleum analysis,[25] environmental organic matter,[26] porphyrins in coal,[27] and porphyrins in heavy oil[28] are also available. Therefore, we highlight separation techniques in addition to advances made in porphyrin research facilitated by chemical information provided by mass spectrometric techniques and highlight specific advancements made by ultrahigh resolution FT-ICR mass analyzers; we do not intend this to be comprehensive for all analytical techniques applied for petroporphyrin characterization.

Special Issue: 2021 Pioneers in Energy Research: Alan Marshall

Received: June 18, 2021
Revised: July 28, 2021

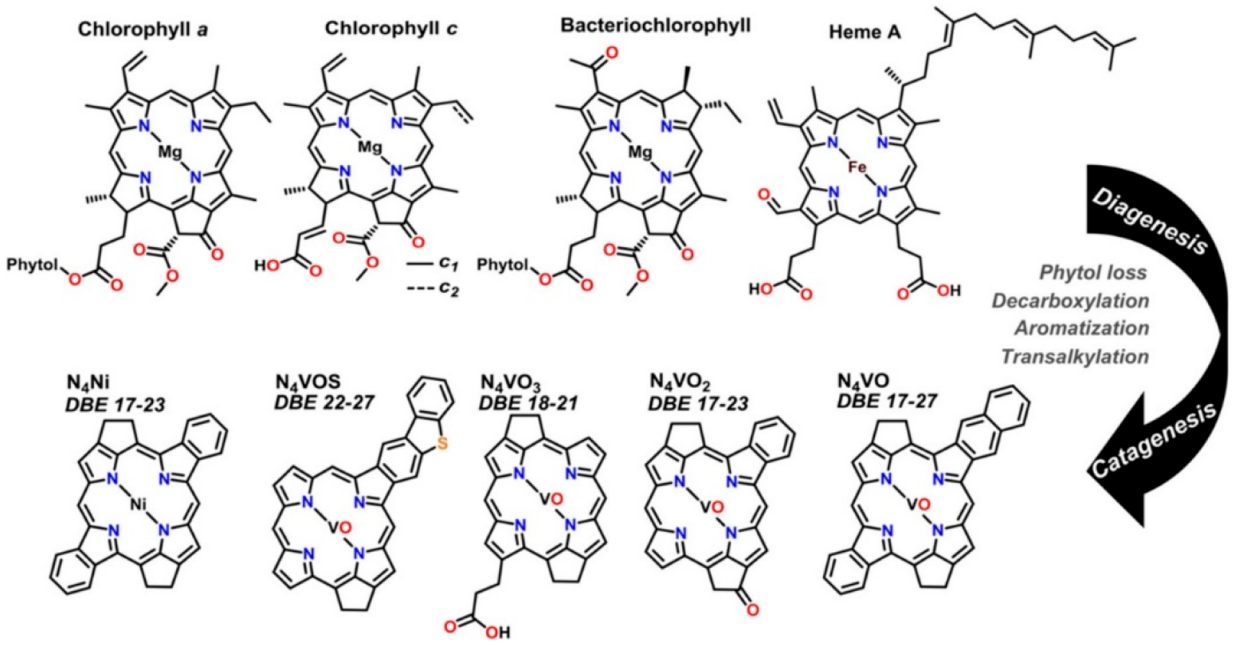

Figure 1. Geochemical transformations of chlorophylls. Diagenesis involves phytol loss, decarboxylation, aromatization, metalation/demetalation, and heteroatom insertion; catagenesis involves thermally induced transalkylation and degradation.[16] Reproduced from ref 13: Ramirez-Pradilla, J. S.; Blanco-Tirado, C.; Hubert-Roux, M.; Giusti, P.; Afonso, C.; Combariza, M. Y. Comprehensive petroporphyrin identification in crude oils using highly selective electron transfer reactions in MALDI-FTICR-MS. *Energy Fuels* **2019**, *33*, (5), 3899−3907. Copyright 2019 American Chemical Society.

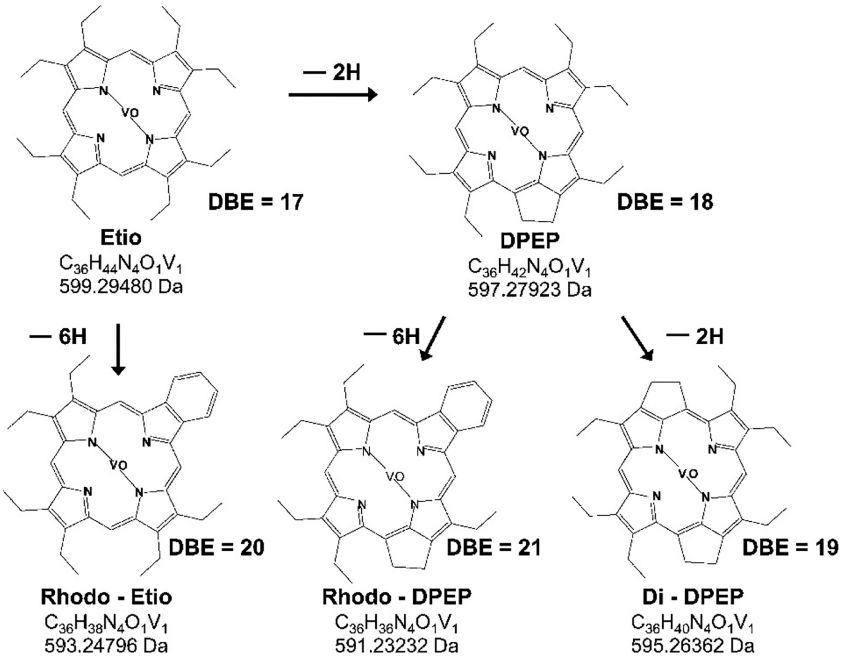

Figure 2. Proposed structures of petroporphyrins according to their number of unsaturation (DBE = $C - h/2 + n/2 + 1$) calculated from their molecular formula based on accurate mass measurements.[29,30] Reproduced from ref 30: McKenna, A. M.; Purcell, J. M.; Rodgers, R. P.; Marshall, A. G. Identification of vanadyl porphyrins in a heavy crude oil and raw asphaltene by atmospheric pressure photoionization Fourier transform ion cyclotron resonance (FT-ICR) mass spectrometry. *Energy Fuels* **2009**, *23*, (4), 2122−2128. Copyright 2009 American Chemical Society.

In 2001, electrospray ionization coupled to Fourier transform ion cyclotron resonance mass spectrometry (FT-ICR MS) first identified petroporphyrins at the molecular formulas leve, and provided elemental composition assignments for identified vanadyl porphyrins.[29] Advances in high resolution mass analyzers provided new discoveries in petroporphyrins compounds, including the molecular level characterizations of vanadyl, nickel, iron, and gallium porphyrins in petroleum, shale oil, biofuels, and natural petroleum seeps.[21,30−41]

Petroporphyrin Structural Elucidation. *Collisional Cross Section.* Although mass spectrometry can provide molecular formula information that is used to propose core

https://doi.org/10.1021/acs.energyfuels.1c02002
Energy Fuels XXXX, XXX, XXX−XXX

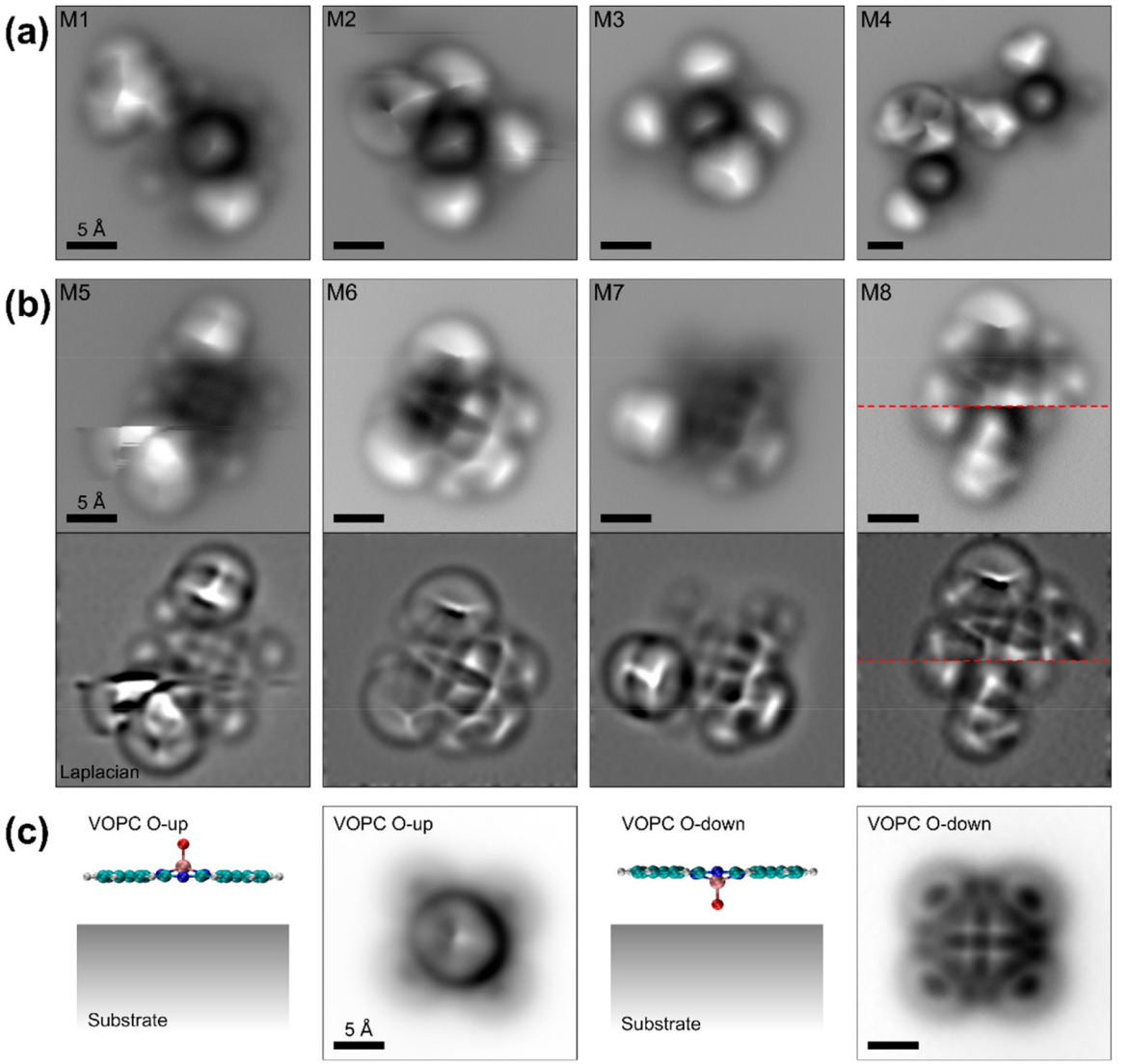

Figure 3. (a) Constant-height AFM images with CO-functionalized tips of petroporphyrins with a strongly repulsive center. (b) Constant-height AFM images with CO-functionalized tips and corresponding Laplace-filtered images of petroporphyrins where atomic resolution of the porphyrin core was achieved. Note that the image of compound M8 is composed of two AFM scans taken at different tip−sample distances, where the scan shown in the lower half was taken at a 1.4 Å larger tip height than the upper half. (c) Schematic representation and corresponding AFM images of the two different adsorption positions observed for vanadyl phthalocyanine. Reproduced from ref 21: Zhang, Y.; Schulz, F.; McKay Rytting, B.; Walters, C. C.; Kaiser, K.; Metz, J. N.; Harper, M. R.; Merchant, S. S.; Mennito, A. S.; Qian, K.; Kushnerick, J. D.; Kilpatrick, P. K.; Gross, L. Elucidating the geometric substitution of petroporphyrins by spectroscopic analysis and atomic force microscopy molecular imaging. *Energy Fuels* **2019**, *33*, 6088−6097.

structures based on the general porphyrin tetrapyrrolic macrocycles (Figure 2), it cannot differentiate structural isomers. One method that can provide separation of structural isomers based on collisional cross sections is ion mobility mass spectrometry (IMS).[7,42] IMS is a gas-phase separation technique that separates ions by molecular size and shape and determines an ion collision cross section (CCS) based on drift time, an intrinsic property of the ion. The CCS of an ion can be predicted based on tridimensional structures obtained from molecular modeling.[43] Due to timing incompatibilities, only a few IMS techniques can be associated with FT-ICR MS detection.[44] In particular, high-field asymmetric-waveform ion-mobility spectrometry (FAIMS) and trapped ion mobility spectrometry (TIMS) are IMS techniques for which the IMS separation can be adjusted to the scan speed of the FT-ICR mass analyzer.[44−46] Compared to FAIMS, TIMS is a low field IMS separation that allows derivation of CCS values from experimental results.[47] Despite a lower resolving power compared to FT-ICR mass detectors, time-of-flight MS presents an advantage due to fast acquisition speed. For example, Zheng et al.[22] combined positive-ion ESI with TIMS-TOF-MS to investigate petroporphyrins aggregates from porphyrin-enriched crude oil fractions.[48] TIMS-FT-ICR MS was first applied to the characterization of synthetic geologically relevant metalloporphyrins by Benigni et al.,[49] who reported octaethylporphyrin as protonated and cationized forms with Mn, Ni, Zn, VO, and TiO_2 based on experimental CCS combined with theoretical DFT calculations. Recently, Maillard et al. applied APPI-TIMS-FT-ICR MS to determine CCS of vanadyl porphyrins from asphaltenes derived from Athabasca bitumen and observed a linear correlation between CCS and carbon number at the same DBE.[50] This indicates

https://doi.org/10.1021/acs.energyfuels.1c02002
Energy Fuels XXXX, XXX, XXX−XXX

that for a specific core molecular structure, the extent of alkylation results in a linear change in CCS and can be used to estimate the CCS for putative petroporphyrins cores with no alkyl substituents. Lastly, theoretical CCS determinations were conducted based on core structures and extrapolated to alkylated petroporphyrins based on the observed linear correlation between CCS and degree of alkylation.[50] On the basis of DFT theoretical calculation, putative structures with theoretical CCS that correlate to experimental values have been proposed.

Atomic Force Microscopy. Recently, the molecular structures of petroporphyrins were reported through a combined technique approach of ultraviolet−visible spectroscopy, FT-ICR MS, and noncontact atomic force microscopy (AFM).[21] Surprisingly, the authors report evidence of one or a few β hydrogens present in low carbon number porphyrins, which support dealkylation under catagenesis. Figure 3 shows constant-height atomic force microscopy images of petroporphyrins (M1, M2, M3, and M4), and all exhibit a very repulsive feature in the center, which prevents the AFM tip from approaching the molecule closely enough to resolve the porphyrin core. In addition, several side groups can be observed, with a varying degree of bulkiness.[21]

Tandem Mass Spectrometry. Tandem mass spectrometry has been used for many years to obtain detailed structural information from specifically selected ions. MS/MS involves ion selection using a first mass analyzer, typically a quadrupole followed by ion activation by collision or through IR or UV light irradiation. With a FTICR mass analyzer, it is also possible to perform ultrahigh resolution in-cell ion isolation on the order of a single mass-to-charge ratio that can be fragmented with infrared multiphoton dissociation (IRMPD).[51] In 1986 and 1989, Yost and co-workers demonstrated the interest of tandem mass spectrometry with electron ionization to evidence the extent of alkylation of geoporphyrins obtained after TLC fractionation.[52,53] Beato et al.[54] used tandem mass spectrometry to characterize geoporphyrins from bitumen and kerogen showing that the peripheral substituents of Ni(II) and VO(II) porphyrins of the same carbon number are similar.[54] Laycock et al.[55] demonstrated that the (M−43)+, (M−44)+, and (M−45)+ product ions are particularly useful for distinguishing the skeletal type of cycloalkanoporphyrin. Van Berkel et al. used MS/MS with NH_3 chemical ionization to characterize geoporphyrins.[56] In 1999, Rosell-Melé et al.[57] used liquid chromatography tandem mass spectrometry to measure porphyrins from oil shales after a demetalation step. The incorporation of online chromatographic separation limited challenging isobaric interferences. Woltering et al.[58] recently applied LC-MS^n with a hybrid ion trap-Orbitrap instrument to characterize Ni, VO, Cu, Zn, and Mn geoporphyrins and combined with multistage mass spectrometry accurately identified greater than C_{33} porphyrin structures with extended alkyl side chains.[58]

METHODS FOR EXTRACTION AND PURIFICATION OF METALLOPORPHYRINS

In general, the separation strategies for vanadyl porphyrins comprise solvent extraction (e.g., liquid/liquid and extrography), chromatographic methods (e.g., selective affinity HPLC, thin layer chromatography, and silica gel column chromatography), supercritical fluid extraction, and novel/prospective methods such as molecular imprinted polymers. We categorize these methods and highlight noteworthy contributions that have furthered mass spectral detection of porphyrins below.

Solvent Extraction: Solid/Liquid and Liquid/Liquid Extraction and Extrography. Xu et al.[59] first isolated vanadyl and nickel porphyrins from two Chinese heavy crudes that were purified by silica gel chromatography, demetallized with methyl sulfonic acid, and analyzed by LDI TOF-MS. Here, extrography isolated crude oil fractions enriched in vanadyl porphyrins (methanol extraction) and nickel porphyrins (acetonitrile extraction) based on adsorption on diatomite followed by Soxhlet extraction and further purified with an eluotropic gradient of cyclohexane/dichloromethane/chloroform.[59] LDI TOF-MS identified Etio porphyrins with a carbon number ranging between C_{26}−C_{40} in fractions of purified VO and Ni porphyrins. Liu et al.[60] further extended porphyrin characterization with silica gel chromatography fractions of Chinese heavy oil and simultaneously detected vanadyl porphyrins, sulfur-containing vanadyl porphyrins, oxygen-containing vanadyl porphyrins, and nickel porphyrins by positive-ion ESI FT-ICR MS and surprisingly detected nickel porphyrins as radical cations ($M^{+\bullet}$). The authors attribute stable radical cation formation in positive-ion ESI (as previously observed by Rodgers et al.[29]) to the low oxidation potential of nickel porphyrins. Another study sequentially fractionated Venezuelan Orinoco heavy crude by extrography and silica gel column chromatography into subfractions that were characterized by ESI FT-ICR MS, and identified three new types of vanadyl porphyrins corresponding to $C_nH_mN_4VO_2$, $C_nH_mN_4VO_3$, and $C_nH_mN_4VO_4$.[35] Based on aromaticity calculated as double bond equivalents (DBE = number of rings plus double bonds to carbon, DBE = $C - h/2 + n/2 + 1$, calculated from elemental composition $C_cH_hN_nO_oS_s$),[61] the authors report oxygen incorporation into porphyrin core structures as ketone/aldehyde and carboxylic acid moieties.[35]

Liu et al.[60] reported the isolation of vanadium compounds by extrography and silica gel open column chromatography with methanol, dimethylformamide, and toluene for hydrotreated products that were further separated into subfractions through silica gel chromatography and an elutropic gradient composed of cyclohexane, dichloromethane, and methanol. Positive-ion ESI FT-ICR MS identified vanadium compounds in toluene extracts as the most resistant for hydrotreating, and the vanadium compounds in the methanol extract, primarily as $C_nH_mN_4V_1O_1$, were removed through hydrotreating due to side-chain cracking.[62] Chauhan and de Klerk[63] reported the extraction of vanadium and nickel from diluted oil sands bitumen with (hydrochloric-acidified, aqueous sodium chloride, and water-diluted) ionic liquids and investigated the dissociation equilibria differences and partitioning of vanadium and nickel extraction and suggested improved extraction of nickel porphyrins with HCl acidification, dilution with aqueous NaCl, and dilution with water. Gascon et al.[64] reported for the first time the gel permeation chromatography (GPC) separation of vanadium and nickel species found in maltenes. Here, maltenes were extracted with methanol, acetonitrile, and dimethylformamide and subsequently separated by GPC with tetrahydrofuran as the mobile phase, which separates petroleum fractions into high molecular weight (HMW), medium molecular weight (MMW), and low molecular weight (LMW) fractions. The authors hypothesize that the final fraction is enriched in disaggregated/free molecules, whereas

https://doi.org/10.1021/acs.energyfuels.1c02002
Energy Fuels XXXX, XXX, XXX−XXX

the HMW consists of highly aggregated species, and conclude that liquid−liquid extraction of maltenes with acetonitrile selectively removed low molecular weight vanadium compounds, whereas dimethylformamide extracted low and medium molecular weight species from the high molecular weight species that remain in the maltene remnant.[64] Notably, the authors demonstrate the separation of three distinctive fractions of vanadium and nickel compounds in maltenes based on molecular weight and aggregation tendency determined by GPC.[13] The same authors did a similar study applied directly to asphaltene using successive extraction with dimethylformamide, acetone, and finally acetonitrile. Again, two highly aggregated enriched porphyrins fractions were hypothesized in DMF and an acetone fraction by GPC. A part of disaggregates/free porphyrins were hypothesized in the last ACN fraction. This methanol and ACN extract from maltene and asphaltene are corresponding to 45% and 5%, respectively, of the total V compounds showing that most of the V porphyrins are underaggregated forms in crude oil samples.

Supercritical Fluid Extraction and Fractionation (SFEF). Supercritical fluid extraction separates heavy oil into fractions, which can then be further characterized for porphyrins. Supercritical fluid extraction applied to vacuum residues derived from an extra-heavy crude oil (Venezuelan Orinoco) separates residue species based on molecular weight and degree of molecular condensation.[65] The authors identified a series of compounds with the most abundant peak with $m/z \sim 530$ detected by +APPI FT-ICR MS in the SFEF endcut, which also contained for ∼70 wt % C_7 asphaltenes. These compounds corresponded to vanadyl porphyrins with DBE values between 17 and 21.

CHROMATOGRAPHIC FRACTIONATION OF METALLOPORPHYRINS

Chromatographic separation and purification methods applied to petroporphyrins are detailed below.

Selective Affinity Chromatography. A portion of the metalloporphyrin fraction isolated from asphaltenes through reactive modification and affinity chromatography through derivatization of vanadyl porphyrin targets was reported by Yin et al.[66] This method reports modification of vanadyl porphyrin complexes through reaction with oxalyl chloride followed by long-chain alkylamine or perfluoroalkyl-amiline to yield an imdio vanadium derivative containing octadecyl or perfluorooctyl side chains. Derivatized vanadium-containing porphyrins were selectively isolated by affinity column chromatography with C_{18}-silica gel or perfluorous ($-C_8F_{17}$) silica gel. The authors report the removal of tagged metalloporphyrins from petroleum asphaltenes, with a mass recovery of ∼15%−40% of total vanadium and nickel content with minimal asphaltene loss.[67]

Size-Exclusion Chromatography/Gel Permeation Chromatography. Acevedo et al.[68] detailed microsized exclusion chromatography coupled to a mass spectrometer with an inductively coupled plasma ion source (μSEC-HR ICP MS or μSEC ICP) to analyze metals in four asphaltene fractions. Trapped petroporphyrins were characterized from three fractions derived from three separate asphaltene samples from Boscan, Cerro Negro, and Furrial crudes: A1 (toluene insoluble), A2 (toluene soluble), and TC (trapped compounds).[68] Nickel porphyrins were distributed in nearly all types of asphaltene aggregates (toluene insoluble, toluene soluble, and heptane-soluble fractions), and overlapping SEC chromatograms were reported with sulfur for all vanadium and nickel profiles at retention times below the exclusion limit, which indicates that metalloporphyrins are interlocked with asphaltene species and form aggregates in solution, in agreement with previous simulations.[12,68,69]

Gel Permeation Chromatography. Desprez et al.[70] first studied trend correlation between sulfur fraction retention times, distillation cut temperature with boiling points below 560 °C, viscosity, and proportions of trapped sulfur-containing compounds through gel permeation chromatography (GPC) with inductively coupled plasma high resolution mass spectrometry (ICP HR MS). Sulfur, vanadium, and nickel compounds from four crude oils, residues, and SARA fractions were further determined based on GCP ICP HR MS and revealed trimodal distributions in crude oils, resins, and residues.[70] Interestingly, asphaltenes were enriched in highly aggregated Ni-/V-containing compounds (HMW fraction), whereas resins contained higher amounts of MMW and LMW species.[71] Analysis of gel permeation chromatographic (GPC) fractions from an asphaltene sample by direct-infusion FT-ICR MS highlights an inverse correlation of asphaltene aggregate size and aromaticity but was limited due to the low ionization efficiency of larger, aliphatic compounds.[72] In other words, the compositional range (DBE and carbon number) for HMW species revealed abundant species with DBE < 20 and up to C_{50}. Conversely, the LMW/disaggregated material contained a high relative abundance of molecules with DBE > 15 with aromaticity near the polycyclic aromatic hydrocarbon planar limit.[73] GPC separation with online detection by positive-ion APPI FT-ICR MS highlights the presence of highly abundant, aliphatic asphaltene aggregates. Furthermore, the authors report that the composition of vanadyl porphyrins eluting in the most aggregated region span the largest carbon number range. As aggregation decreases, the carbon number range narrows, and the average H/C ratio decreases to almost 1.0, corresponding to porphyrin species with minimal alkyl-chain pendant groups.[74] Additional studies have highlighted the impact of GPC on porphyrin characterization in heavy oil[68,70−72,74−79] and applied GPC to understand hydrodemetallization and hydrodesulfurization processes.[80]

High-Performance Thin-Layer Chromatography. Moulian et al.[81] studied the contribution of porphyrins to asphaltene aggregation and reported that asphaltene aggregate molecular weight increased with the presence of metalloporphyrins that interacted with asphaltene aggregate surfaces, and these species likely play a critical role in asphaltene aggregation, coprecipitation, and demetalation processes. Importantly, this study directly implicates porphyrins in stabilization of noncovalent asphaltene aggregates, in agreement with simulations reported more than a decade prior.[12,82] Additionally, the authors studied porphyrins from asphaltene fractions enriched in single-core/island motifs (acetone extrography fraction) and multicore/archipelago structures (Tol/THF/MeOH extrography fraction), obtained as reported elsewhere.[83−85] The authors separated porphyrins from the extrography fractions by thin-layer chromatography using cellulose as the stationary phase and DCM/MeOH as the eluent, which yielded a continuous elution profile with two prominent TLC fractions: noneluted (highly polar) and eluted. Characterization by laser ablation inductively coupled plasma mass spectrometry demonstrated the existence of abundant V-containing compounds in the TLC subfractions from the asphaltene extrography fractions. In particular, the acetone

https://doi.org/10.1021/acs.energyfuels.1c02002
Energy Fuels XXXX, XXX, XXX−XXX

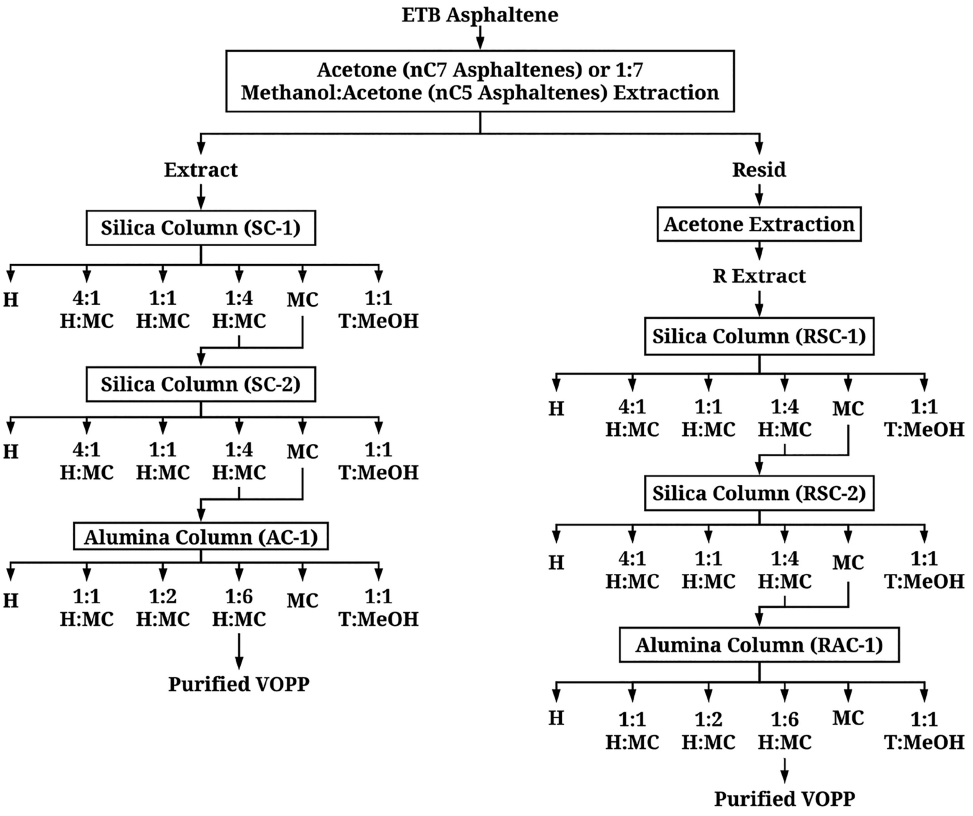

Figure 4. ETB asphaltene VOPP enrichment procedure. Here, ETB is subjected to an extraction, which produces an extract and a residuum. The extract is further fractionated on a silica column (SC-1) using a series of solvents shown below the silica column, including hexane (H), hexane:methylene chloride mixtures (H:MC), methylene chloride (MC), and toluene:methanol mixtures (T:MeOH). The 1:4 H:MC and MC eluents are combined and further fractionated on an additional silica column (SC-2). Again, the 1:4 H:MC and MC eluents from SC-2 are combined and further fractionated on an alumina column (AC-1), where the 1:6 H:MC eluent contained purified VOPPs. The residuum from the original extraction is also further fractionated on several columns, which are named with an R prefix to specify that they are using the residuum from the original extraction.[95,96] Reproduced from ref 95: Rytting, B. M.; Singh, I. D.; Kilpatrick, P. K.; Harper, M. R.; Mennito, A. S.; Zhang, Y. Ultrahigh-purity vanadyl petroporphyrins. *Energy Fuels* **2018**, *32*, (5), 5711−5724. Copyright 2018 American Chemical Society.

fraction revealed abundant V-containing compounds in the eluted fraction, whereas Tol/THF/MeOH was enriched noneluted species. However, molecular-level characterization via MALDI FT-ICR MS revealed vanadyl porphyrins for only the eluted TLC fraction for acetone.[81] The combination of molecular-level (FT-ICR MS) and elemental analyses (ICP-MS) proved that abundant porphyrins are inaccessible to FT-ICR MS because of matrix effects and ionization efficiencies.[81] Importantly, these porphyrins are contained in asphaltene fractions that contain abundant archipelago asphaltenes, which experience a disproportional aggregation tendency than island structural motifs. Furthermore, Moulian et al.[81] presents a method to separate free porphyrins from asphaltenes based on high-performance thin-layer chromatography (HPTLC).

Ramírez-Pradilla et al.[13] reported liquid−liquid extraction of crude oil with acetonitrile and obtained fractions enriched with vanadium and nickel, followed by a purification by high-performance thin-layer chromatography fractionation (HPTLC, aminopropyl-bonded silica) using DCM as the eluent.[13] The authors apply a novel MALDI matrix that favors electron-transfer reactions[86,87] coupled to molecular-level FT-ICR MS and simultaneously detect 518 molecular formulas (the highest number of Ni, VO, oxygenated, and sulfur-containing porphyrins to date) in a single crude oil sample with MALDI FT-ICR MS. Interestingly, S-containing vanadyl porphyrins contain six more DBE compared to porphyrins with no sulfur, consistent with earlier reports.[30]

Microwave Irradiation. Several studies indicate the agreement in the literature that a fraction of vanadium is locked into asphaltene aggregates and remains inaccessible through many techniques, including UV−vis spectroscopy.[88,89] One method proposes separation of porphyrins from asphaltene aggregates from Canadian oil sands bitumen through polar solvent mixtures (e.g., methanol/toluene) and microwave irradiation,[90] previously reported to clean plugged horizontal wellbores and demulsification.[91,92] Fan et al.[90] report rapid asphaltene separation into soluble and insoluble fractions by microwave irradiation, with the soluble material containing abundant vanadyl porphyrins. Asphaltene samples after microwave treatment exhibit a more prominent Soret band compared to without microwave treatment. The authors report poor release of nickel porphyrins compared to vanadyl and conclude that the disproportionate selectivity for the release of vanadyl porphyrins is due to the efficient absorption of microwave irradiation by the vanadyl (V═O) group. The proposed mechanism for vanadyl porphyrin release is based on the formation of asphaltene vesicles in polar solvent mixtures (e.g, toluene/methanol). Early studies have also implicated porphyrins in asphaltene aggregate stabilization.[93,94]

https://doi.org/10.1021/acs.energyfuels.1c02002
Energy Fuels XXXX, XXX, XXX−XXX

PURIFICATION OF METALLOPORPHYRINS

Ultrahigh Purification of Petroporphyrins. Rytting et al.[95] report a method for producing ultrahigh purity vanadyl porphyrin fractions from heavy crude and bitumen to enable characterization and inclusion into model studies of asphaltene−petroporphyrin intermolecular interactions. Fractions are prepared through Soxhlet extraction to yield a porphyrin-rich fraction that is further purified by three consecutive separation steps based on extrography on silica-packed columns and chromatography on alumina-packed columns (Figure 4). The extensive separation method yields purified porphyrins that can be further purified (>85% petroporphyrins by weight) with temperature and centrifugation to yield solubility fractions and highlights the complexity of the purification process, often taking several weeks to obtain a few milligrams of purified petroporphyrin material.[95] Furthermore, purified porphyrins are characterized by small-angle neutron scattering. The collective results suggest a central role in asphaltene aggregation and interfacial film formation dependent on porphyrin structure[96] and interfacial film formation.[97] More functionalized porphyrins that contain sulfur and several oxygen atoms promote asphaltene flocculation at low temperatures, as polyfunctionality enables multiple intermolecular interactions with neighboring asphaltene molecules. Both synthetic and extracted highly functionalized porphyrins promote asphaltene flocculation, whereas simpler porphyrins disrupt asphaltene aggregation.[96]

Sulfocationite Isolation. Recent novel separation methods to purify porphyrins from heavy oil have been investigated and show promise for expanding the compositional knowledge of porphyrin composition. Mironov et al. developed a method for chromatographic preparation of high-purity vanadyl porphyrins based on a sulfuric acid cation exchanger readily prepared from silica gel and sulfuric acid.[98] With a silica gel/sulfuric acid/water weight ratio of 60/15/25, up to ∼50% of vanadyl porphyrins pass through the column with no retention, whereas nonporphyrin impurities are retained on the stationary phase.[98] Vanadyl porphyrins isolated from asphaltenes derived from a heavy oil from the Volga-Ural basin were purified based on a novel strong acid cation-exchange resin and asphaltene sulfocationite method.[99] Subsequent characterization of purified porphyrins by MALDI ToF-MS showed that the composition of isolated vanadyl porphyrins was dependent on the chemical nature of sulfocationite. Furthermore, purification of asphaltene sulfocationite resulted in a 1.1−1.9-fold increase in non-DPEP vanadyl porphyrin structures.[99] Application of the sulfocationite porphyrin purification method to resins and asphaltenes from three heavy oils of different origins and vanadium contents combined with MALDI TOF-MS identified DPE, Etio, Di-DPEP, and Rhodo-DPEP vanadyl porphyrins across all samples, with resins and asphaltenes of the same oil containing significant differences in group compositions of purified vanadyl porphyrins.[100]

IONIZATION TECHNIQUES FOR MS OF METALLOPORPHYRINS

Electron Impact Ionization of Metalloporphyrins. Electron impact ionization, a hard ionization method, is not suitable for the analysis of vanadyl and nickel porphyrins given the low volatility of these species and the high internal energy post ionization, which results in the fragmentation of pendant side groups. Nevertheless, the tetrapyrrole core is stable (not fragmented) even when ionized with high energy electrons (70 eV), which is revealed by native vanadyl/nickel porphyrins and their demetallized forms. Grigsby and Green early reported the characterization of a vanadium-enriched fraction from the >700 °C residue from Cerro Negro heavy oil by low-eV HRMS.[101] The V-enriched fraction was obtained by liquid chromatography and shown to contain 19,500 ppm vanadium. Low-eV HRMS was assisted by sample introduction via probe microdistillation, as it enables the characterization of aromatic and polarizable species in low-volatility mixtures. The mass spectrometry analysis of the generated ions was performed by a high-resolution TOF. The authors concluded that the most abundant V-containing compounds were etioporphyrins with molecular weights between m/z 487−879. The presence of porphyrins was also determined with cyclo-alkyl/aromatic pendant groups with hydrogen deficiency or Z numbers between −32 and −50 ($Z = -2(\mathrm{DBE}) + n + 2$, in which n is the number of nitrogen atoms).[101,102]

Soft ionization methods such as ESI, APCI, and APPI have shown promising results for the intact ionization of nickel/vanadyl porphyrins. However, APCI still suffers some degree of fragmentation, which is believed to be the result of collision of molecules at atmospheric pressure.[103,104]

Electrospray Ionization (ESI) of Metalloporphyrins. Rodgers et al.[29] first applied positive ion ESI FT-ICR MS to identify metalloporphyrins in a Venezuelan heavy oil (Cerro Negro), isolated via column chromatography. The authors found predominance of the dimeric forms of vanadyl and nickel porphyrins, which were dissociated with minimal covalent bond fragmentation, by infrared multiphoton dissociation (IRMPD).[29] Ionization conditions (concentration, solvents, ESI needle voltage), ion transferring from the source to the ICR cell, and FT-ICR MS excitation/detection were optimized in subsequent studies. Thus, the prevalence of porphyrin dimers was not noted in further works.

Electrochemical oxidation in ESI FT-ICR MS improved detection of nickel and vanadyl porphyrins in porphyrin-enriched residue fractions and identified nickel porphyrins.[33] Chen et al.[105] developed a method to enhance the response of nickel porphyrins in ESI by introducing the electrochemical oxidation reaction. Under optimized conditions, nickel and vanadyl porphyrins can be directly ionized as molecular radical cations ($[M]^{+\bullet}$) via electrochemical oxidation due to low oxidation potential and gas-phase ionization energy.[105] This method is capable of direct analysis of both nickel and vanadyl porphyrins in a vacuum residue without any prior sample preparation.[105]

Atmospheric Pressure Photoionization (APPI) of Metalloporphyrins. Because APPI ionizes both polar and nonpolar compounds (e.g., hydrocarbons and porphyrins) in the gas phase simultaneously and can produce both radical ions and protonated/deprotonated ions, the resultant mass spectrum is more complex with up to five times the number of peaks compared to electrospray ionization. The number of mass spectral peaks detected increases in a more complex mass spectrum.[106,107] APPI was first coupled to FT-ICR MS for heavy oil characterization and first characterized a nonpolar species South America in 2006−2007.[106−110] Vanadyl porphyrins and sulfur-containing vanadyl porphyrins were first identified in a fractionation asphaltene sample, and a concurrent increase in DBE and carbon number can occur through benzene and naphthene addition as exocyclic pendant groups in the porphyrin ring structures.[111] Qian et al.[37] further

https://doi.org/10.1021/acs.energyfuels.1c02002
Energy Fuels XXXX, XXX, XXX−XXX

reported a wide diversity of petroporphyrin structures that contain multiple sulfur and oxygen atoms ($C_cH_{2c+z}N_4VO_oS_s$) in vacuum residue by APPI FT-ICR MS.[37] The first comprehensive characterization of vanadyl porphyrins in unfractionated heavy petroleum and virgin asphaltenes by APPI FT-ICR MS was performed by McKenna et al.[30] The authors highlight the need of FT-ICR MS to achieve an unambiguous molecular formula assignment (<300 ppb) and demonstrate the likelihood of misassigning vanadyl porphyrin peaks ($N_4O_1{}^{51}V1$ class) as high DBE O_2 compounds. Vanadyl porphyrins were detected as radical cations $M^{+\bullet}$ and protonated molecules $[M + H]^+$. Trends in the abundance of specific homologous series accounted for the structural diversity of vanadyl porphyrins in heavy crudes and asphaltenes. For example, the identified alkyl-substituted $N_4O_1V_1$ species in Athabasca bitumen asphaltenes revealed DBE values from 16, which corresponds to the tetrapyrrole core, to 23, which suggests the presence of several naphthenic rings or aromatic moieties as side groups.[30]

Vanadyl porphyrins have been detected in asphaltenes isolated from vacuum gas oil distillate cuts, and in pentane, in between C_5–C_7 asphaltenes, and heptane asphaltenes by APPI FT-ICR MS.[112,113] Additional studies apply APPI FT-ICR MS of asphaltene extrography fractions and highlight structural characterization by infrared multiphoton dissociation (IRMPD), confirming the dominance of single core vanadyl porphyrins structures.[83] Supercritical fluid extraction and fractionation (SFEF) of Venezuelan Orinoco extra heavy crude vacuum residue concentrates vanadyl porphyrins in high boiling endcuts detected by APPI FT-ICR MS.[65] Furthermore, Chacón-Patiño et al.[114] investigated the molecular composition of vanadyl porphyrins in PetroPhase 2017 asphaltenes and extrography fractions, with specific focus on molecular composition of vanadyl porphyrins as a function of aggregate size distribution by GPC ICP-MS and online GPC APPI FT-ICR MS at 21 T (Figure 5). The authors performed quantitative detection of vanadium by GPC ICP-MS and concluded that the majority of the vanadyl porphyrin ions are produced from later eluting GPC fractions (low aggregation LMW part) and found that highly aggregated fractions reveal abundant porphyrins with much longer homologous series than those species from the less aggregated GPC fractions.

Porphyrins from C_5–C_7 asphaltenes isolated from Venezuelan heavy oils and a NIST vanadium crude oil standard show a multimodal distribution for the boiling point ranges of vanadium-containing compounds (Figure 6a).[113] Positive ion APPI FT-ICR MS revealed that the molecular composition of vanadyl and nickel porphyrins is multimodal in terms of aromaticity (DBE). For example, $N_4O_1V_1$ and $N_4O_2V_1$ classes comprised dominant homologous series with DBE < 22. However, when sulfur was present, for example, $N_4O_1S_1V_1$ class, the composition shifts toward higher DBE (increase in 4–6 units, Figure 6b). Similarly, nickel porphyrins correspond to two main homologous series and indicate a bimodal molecular structure (Figure 6b), which implicates this chemical characteristic in multimodal distributions of boiling point detected by high temperature gas chromatography (GC) hyphenated with coupled ICP-MS.

Laser Desorption Ionization (LDI) of Metalloporphyrins. Laser desorption ionization (LDI) applied to heavy oil and asphaltenes, enriched in metalloporphyrins, has been controversial due to the prevalence of a noncovalent cluster formation in the desorption plume for complex samples that result in aggregate formation.[59,115] Cho et al.[116] evaluate laser

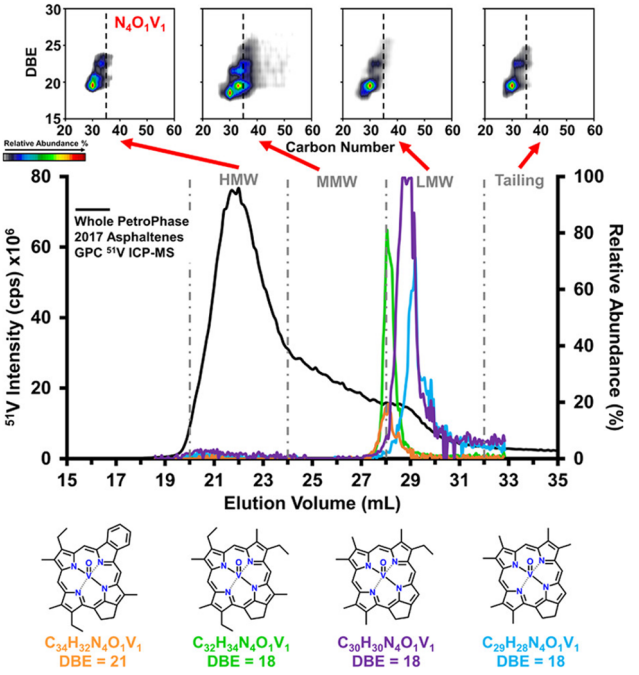

Figure 5. DBE vs carbon number plots for the $N_4O_1{}^{51}V_1$ class for the various GPC regions from whole PetroPhase 2017 asphaltenes (upper panel) and relative abundance as a function of elution volume for the most abundant $N_4O_1{}^{51}V_1$ formulas (middle panel). Data derived from (+)APPI 21 T FT-ICR MS characterization. The GPC ^{51}V ICP–MS chromatogram (black) is included for reference, and the most likely molecular structures for the most abundant vanadyl porphyrins are presented in the lower panel. Reproduced from ref 114: Chacón-Patiño, M. L.; Moulian, R.; Barrère-Mangote, C.; Putman, J. C.; Weisbrod, C. R.; Blakney, G. T.; Bouyssiere, B.; Rodgers, R. P.; Giusti, P. Compositional trends for total vanadium content and vanadyl porphyrins in gel permeation chromatography fractions reveal correlations between asphaltene aggregation and ion production efficiency in atmospheric pressure photoionization. *Energy Fuels* **2020**, *34*, (12), 16158–16172. Copyright 2020 American Chemical Society.

desorption ionization for vanadyl and nickel porphyrins and report five types of VO^{2+} and Ni^{2+} porphyrin complexes (etio, DPEP, rhodo-etio, rhodo-DPEP, and di-DPEP) observed with LDI compared to only three porphyrin complexes by +APPI but report fragmentation of porphyrins due to loss of CH_3 by LDI. Interestingly, Kachadourian et al.[117] found that the number of N-ethyl losses for a series of β-substituted cationic metalloporphyrins depends on the redox state of the metal. The authors suggested fragmentation in LDI as a way to determine the metal oxidation state in metalloporphyrins.[117] Xu et al. combined UV–vis and LDI TOF MS to discriminate vanadyl porphyrins in two Chinese crude oils. A Soret band (406 nm) in the UV–vis spectra of some extracts and MWD between m/z 430 and 580 confirmed the presence of petroporphyrins. Thermal maturity of the crude oil samples was determined using a $\sum$DPEP/$\sum$ETIO ratio.[59] Likewise, porphyrins isolated from a heavy oil residue (500+ °C) of Chinese Gudao heavy crude were characterized by LDI TOF-MS and report nickel porphyrin etio homologues from C_{25}–C_{34+} and based on the $\sum$DPEP/$\sum$ETIO ratio of ∼1.04 conclude that Gudao oil is nearing maturity.[118]

Matrix-Assisted Laser Desorption Ionization (MALDI) of Metalloporphyrins. Alternative charging pathways in MALDI can increase the detection of petroporphyrins to lower

https://doi.org/10.1021/acs.energyfuels.1c02002
Energy Fuels XXXX, XXX, XXX–XXX

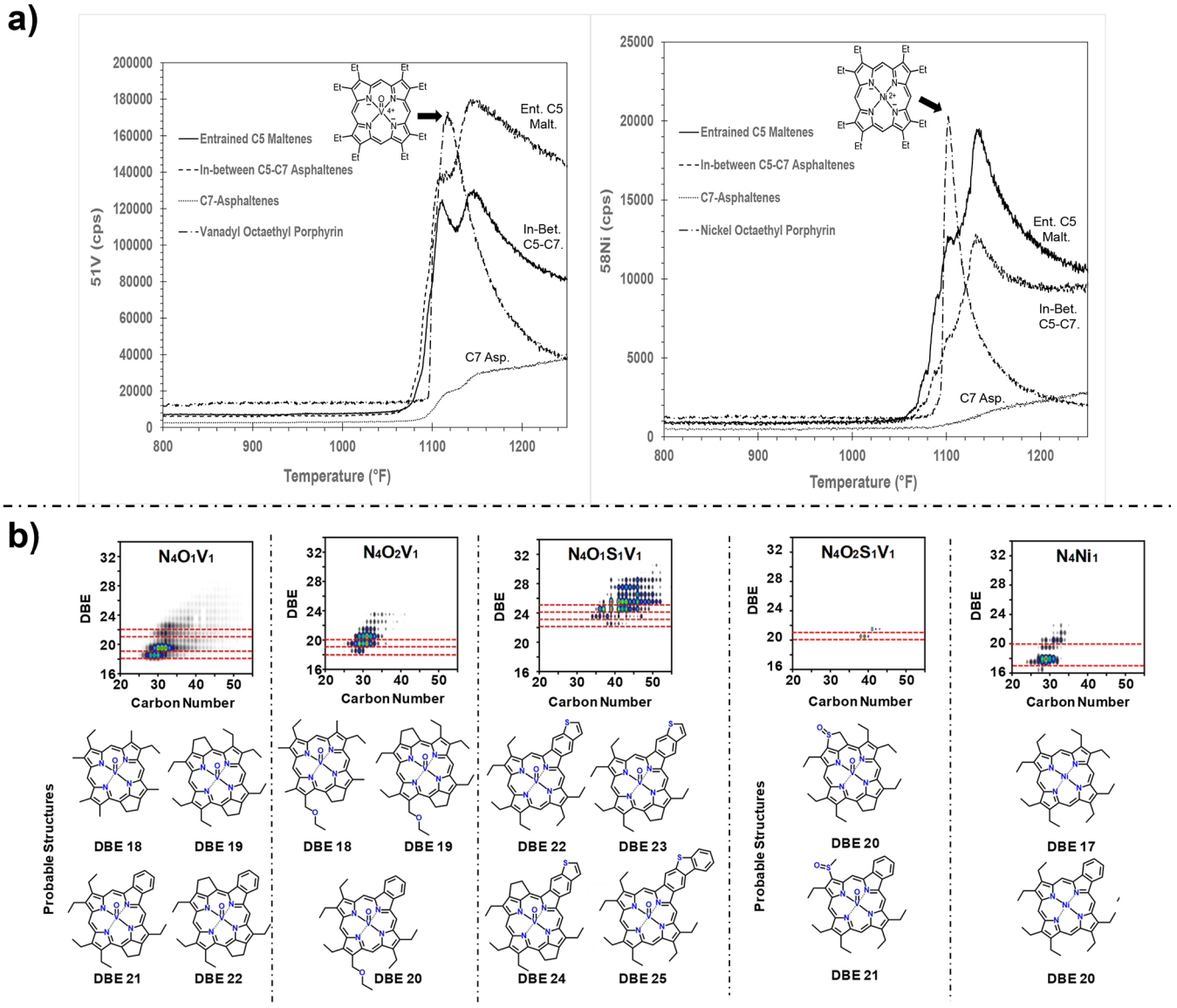

Figure 6. (a) Trace of the vanadium and nickel signals versus boiling temperature (°F) for the entrained C5 maltenes, in between C5−C7 asphaltenes, and C7 asphaltenes for a Venezuelan heavy oil. (b) Isoabundance-contoured plots of DBE vs carbon numbers and probable structures of the vanadium/nickel-containing species for the in between C5−C7 asphaltenes.[113] Reproduced from ref 113: Chacón-Patiño, M. L.; Nelson, J.; Rogel, E.; Hench, K.; Poirier, L.; Lopez-Linares, F.; Ovalles, C. Vanadium and nickel distributions in pentane, in-between C5−C7 asphaltenes, and heptane asphaltenes of heavy crude oils. *Fuel* **2021**, *292*, 120259. Copyright 2021 American Chemical Society.

concentrations compared to infusion ionization techniques (e.g., electrospray ionization, atmospheric pressure photoionization). Electron transfer (ET) secondary reactions in MALDI involve charge transfer between the matrix primary ions (radical cations) and neutral analytes. Thus, the relative ionization energies (IEs) of the species involved determine the reaction's spontaneity. ET is thermodynamically favored when the matrix's IE is higher than the analyte's IE (IEM > IEA).[119] Crude oil molecular complexity results in a broad range of IE values for its components, extending from 6.5 to 12 eV. Interestingly, petroporphyrins exhibit some of the lowest IE values in crude oils due to their highly conjugated, heteroatom-containing aromatic tetrapyrrole cores.[69] Therefore, selective ionization by ET reactions is possible by selecting a matrix with IE above that of the petroporphyrins homologous series while suppressing the ionization of molecules with higher IE than the matrix in the crude oil sample.[120]

Giraldo-Dávila et al.[121] illustrated for the first time the selectivity of the ET approach in the analysis of two South American crude oils. The authors showed that petroporphyrins (IE 6.5−7.0 eV) were selectively ionized as radical cations in a MALDI-TOF instrument using a cyanophenylenevinylene derivative with an IE of 8.2 eV as the matrix.[121] Subsequently, using the ET MALDI approach on a FT-ICR instrument, Ramirez-Pradilla and co-workers[13,120] reported the highest number of Ni, VO, oxygenated, and sulfur-containing porphyrins in a single crude oil sample (868 species total) by liquid−liquid extraction and high-performance thin-layer chromatography fractionation. Petroporphyrins have a low ionization energy (between 6.5 and 7.0 eV), and thus, when combined with high ionization energy matrices, more than 500 different petroporphyrins can be identified since electron-transfer reactions are favored.[121] In contrast with APPI and LDI, the ET MALDI approach not only favors petroporphyrin

https://doi.org/10.1021/acs.energyfuels.1c02002
Energy Fuels XXXX, XXX, XXX−XXX

selective detection it also decreases spectral complexity increasing analytical figures of merit such as S/N and mass accuracy. These effects facilitate ancillary identification strategies for petroporphyrins, such as isotopic fine structure analysis and data refinement with Kendrick mass defect (KMD) plots.

MOLECULAR SIMULATIONS AND COMPUTATIONAL APPROACHES

Porphyrins are part of organo-metallic complexes which were extensively investigated from computational approaches since the early 1990s in order to obtain knowledge on their structures,[122,123] their electronic properties,[124] or their reactivity.[125] As previously pointed out, petroleum metalloporphyrins are primarily vanadyl porphyrins and nickel porphyrins. In this part, we describe the methodologies implemented for the investigation of these porphyrins, the results obtained from these works, and the link with experimental techniques.

Computational Approaches of Metalloporphyrins. First, we describe the needed methodology to investigate metalloporphyrins from computational approaches, and we try to highlight the key features of such systems and their consequence in the choice of a methodology. Theoretical chemistry methodologies can be mainly split in two families, namely, quantum chemistry calculations and molecular mechanics calculations. Both of them aim to provide the energy of a molecular systems using approximations or empirical laws.

Quantum chemistry calculations are based on the resolution of the Schrödinger equation and provide the electronic states of the systems characterized by their wave functions and energies. These methodologies provide a full description of the system considering explicitly the electronic density which open various field of investigation including electronic or optical transitions, electronic transfer, chemical bond analysis and chemical reactivity. But the price of the accuracy of these methodologies is that they are computationally costly. Depending on the required accuracy, they are thus limited to at most a few hundreds of atoms in high performance computing centers. Calculations mainly consist of the implementation of density functional theory calculations (DFT).

On the other side, molecular mechanics aims to provide empirical laws, usually analytic expressions, allowing computation of the energy and forces of a large system with a high efficiency. These laws are called force fields and are usually parametrized against experimental data or quantum chemistry calculations. The efficiency of these calculations allows researchers to implement molecular dynamics simulations along which the trajectories of large or complex systems are integrated over time. Nowadays, simulations of hundreds of thousands of atoms are considered. However, in such approaches, electrons are usually not described explicitly but represented in terms of partial charges, dipoles, or even neglected in some hydrocarbon systems without any heteroatoms.

Molecular Mechanics Methodologies Applied to Metalloporphyrins. In theoretical chemistry, metalloporphyrins and, in particular, petroleum metalloporphyrins (petroporphyrins), are complex systems for several reasons. First, considering the structure, the nucleus of the porphyrin with its four pyrrole rings already counts at about 40 atoms. That may explain why the first studies of nickel porphyrins, in 1991, implemented molecular mechanics methodologies.[126] This work focuses on nickel porphyrins as a cofactor of a reductase enzyme of methanogenic bacteria. Moreover, when considering petroleum porphyrins, the structure of the compounds are still not completely known, in particular, the length and composition of lateral chains crafted on the nucleus. That point is also a bottleneck for computational approaches for which the structure of the system is a starting point and considering a too huge chemical diversity involve a too large computational effort. The next point of complexity concerns the binding of the metal and the porphyrin. The mixture of organic and inorganic compounds needs the convergence of different theoretical formalisms or specific force fields. In the 1990s, the main concern of works on metalloporphyrins addressed the description of the metal−organic bonds in porphyrins.[122,127,128]

The evaluation of metal−organics bond energy was investigated more recently using quantum chemistry calculations.[130] Finally, the accurate description of the electronic structure of metal−organic compounds needs to use an adapted quantum chemistry formalism. In particular, metal elements present *d* electrons that are strongly localized and thus need a methodology able to treat the electronic correlation accurately. Moreover, depending on the oxidation degrees of the metal, metal−organic compounds are generally open-shell systems which may present electronic states of different spin multiplicity in a short energy range. In that scope, vanadyl porphyrins are radicals, and accurate descriptions of the electronic structure of these compounds need to implement multireferences methodologies[129] which are among the heaviest quantum chemistry calculations in terms of computational effort. For example, Figure 7 shows the molecular orbitals of a vanadyl porphyrins. One can see that

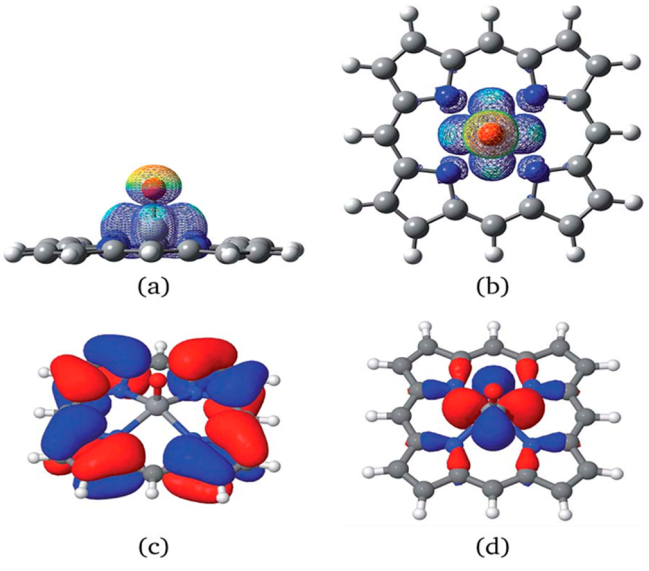

Figure 7. (a, b) Side and top views of the spin electronic density of a vanadyl porphyrin, respectively. (c) HOMO and (d) HOMO-2 molecular orbitals. Reproduced from ref 129: Munoz, G.; Gunessee, B. K.; Bégué, D.; Bouyssiere, B.; Baraille, I.; Vallverdu, G.; Santos Silva, H. Redox activity of nickel and vanadium porphyrins: A possible mechanism behind petroleum genesis and maturation? *RSC Adv.* **2019**, *9*, 9509. and licensed under a Creative Commons Attribution-NonCommercial 3.0 Unported License.[129]

https://doi.org/10.1021/acs.energyfuels.1c02002
Energy Fuels XXXX, XXX, XXX−XXX

the unpaired electron is well localized on the vanadyl group, but the corresponding molecular orbital is not the HOMO orbital which may be a clue of the stability of the radical.

Structure of Metalloporphyrins. The first attempt to consider metalloporphyrins through computational approaches concerns molecular mechanics studies of unique porphyrin molecules.[122,126−128,131] These works mainly address conformational analyses of metalloporphyrins and compare the flat and ruffled conformations of porphyrins as a function of the metal center and substituents crafted on the pyrrolic core. The results came with the first development of reliable force fields able to reproduce the expected conformations. Two main approaches were envisaged to describe the metal−organic bonding. The first one is the point in a sphere model[122,128] where the metal−ligand bond is not explicitly included in the force field. The position of the metal in the porphyrin ring is provided by the size of the metal and the charges of the neighbors. With this choice being not accurate enough, new force fields were developed including explicitly the metal−ligand bond.[127,128,132,133] The force fields were parametrized for 3d row transition metals in general including separately several oxidation degrees or spin states of the metal center and considering crystal structures as target properties.[132] An effort was made to describe both the metal−organic bond inside the porphyrin and with additional ligand molecules.

The first work implementing the quantum mechanical approach by Cundari et al.[134] is also the first one considering vanadyl porphyrins. In this work, molecular mechanics and both semiempirical and Hartree−Fock methodologies to predict the structures of vanadium oxo-complexes are in agreement with experimental structures, and the work provides stretching parameters for V−O and V−N bonds for several vanadium oxidation degrees and oxygen compositions. Later, the ruffling of nickel porphyrins was investigated through DFT calculations.[135] The study includes an analyze of the contribution of the overlap between π molecular orbitals to conformer stability. The proposed structures of nickel porphyrins and associated vibrational spectra computed from DFT calculations were also determined by Raman and IR spectroscopies.[136]

More recently, the conformations of metalloporphyrins and substituted deformations were rationalized thanks to a normal-mode analysis of a crystallographic database.[123] This study provides a global overview over porphyrin conformations linked to metal centers and binding molecules.

Metalloporphryins and Intermolecular Interactions. The intermolecular interactions are the microscopic driving force of global macroscopic behaviors. Following a bottom-up approach, computational approaches are efficient methodologies to increase the knowledge on systems at a macroscopic scale from a microscopic description of the system. On that scope, the accuracies of force fields or quantum chemistry methodologies rely on their capacity to reflect these intermolecular interactions.

A first level is the characterization of the interaction between pairs of compounds including a metal porphyrins. Considering only pairs of compounds or a few numbers of molecules allows implementation of quantum chemistry calculations in order to investigate interactions between metalloporphyrins and resins or asphaltenes model molecules.[69,137−140] In particular, a large effort ensued to understand the contributions of π-stacking interactions,[140] hydrogen bonds,[69,138] or metal−ligand interactions through direct bonding onto the metal center.[69,137,139−141] These studies highlight the driving force of porphyrins behaviors into asphaltene aggregates and the balance between π stacking, hydrogen bonds, and metal coordination. In the case of nickel porphyrins, a consensus is reached about the predominance of the typical association scheme through π-stacking interactions,[138,139] and the axial binding onto the nickel center strongly depends on the electronic state of the nickel.[69] For vanadyl porphyrins, both axial binding and π-stacking interactions are hindered by steric effects and the accessibility of the vanadium atom due to the out of plane conformation of the vanadyl group.[69,138] Therefore, vanadyl porphyrins cannot be found in between asphaltenes molecular planes but rather bridge several nanoaggregates through side-chains interactions and hydrogen bonds.[142]

Moreover, calculations show that asphaltene−asphaltene interaction energies are larger than asphaltene−porphyrin interaction energies, which support the idea that trapped compounds and resins preferentially bond to porphyrins rather than asphaltenes in large aggregates.[138,139] These conclusions were supported by molecular dynamics calculations that take into account solvent effects, asphaltene diversity, and thermodynamics conditions and concluded that metalloporphyrins do not directly affect asphaltene−asphaltene interactions.[138,139,142,143] However, polar lateral chains on porphyrin core structures leads to hydrogen bond interactions with both asphaltenes and water, causing reinforcement of π-stacking interactions between asphaltenes. Therefore, the presence of metalloporphyrins may display an interfacial activity and, depending on the solvent, induces either a stronger precipitation in *n*-heptane or stabilizes aggregate at a water/oil interfaces.[139,142,143]

Several works focus on the interaction between metalloporphyrins and solid surfaces.[144−146] The adsorption onto the surfaces is either undesirable due to side effects on the whole production chain, or required for the conception of sieves or traps of metal compounds. Such calculations implement periodic DFT calculations. A recent review presents a collection of periodic DFT calculations associated with metal porphyrins for various applications.[147] The adsorption of porphyrins and metal porphyrins, in comparison with asphaltene, onto a fully hydroxylated (0001) surface of α-quartz was investigated, and adsorption energies of asphaltene molecules of the same order of magnitude than porphyrins were reported.[146] However, this interaction is lowered for metal porphyrins whatever the metal center.[146]

Reactivity of Porphyrins. In biological systems and more particularly in enzymes, the heme cofactor is the catalytic center of a large number of chemical processes. Several groups investigated the catalytic potential of petroleum-derived metalloporphyrins and their reactivity in crude oil.[129] The binding energies of the metal center and the porphyrins were investigated to assess the stability of the organo-metallic complexes and routes of conversion reactions in catalytic systems.[130,148] Vanadyl porphyrins possess the strongest binding energies followed by nickel and iron.[130]

One reason for the interest in the metal porphyrins reactivity concerns the demetallization steps achieved through hydrodemetallization or hydrotreating, as reported for nickel porphyrins and vanadyl porphyrins.[149,150] DFT calculations contributed to determining the more likely pathways for the hydrogenation of nickel porphyrins and the detection of the intermediate.[149] The results indicate that best catalysts may

https://doi.org/10.1021/acs.energyfuels.1c02002
Energy Fuels XXXX, XXX, XXX−XXX

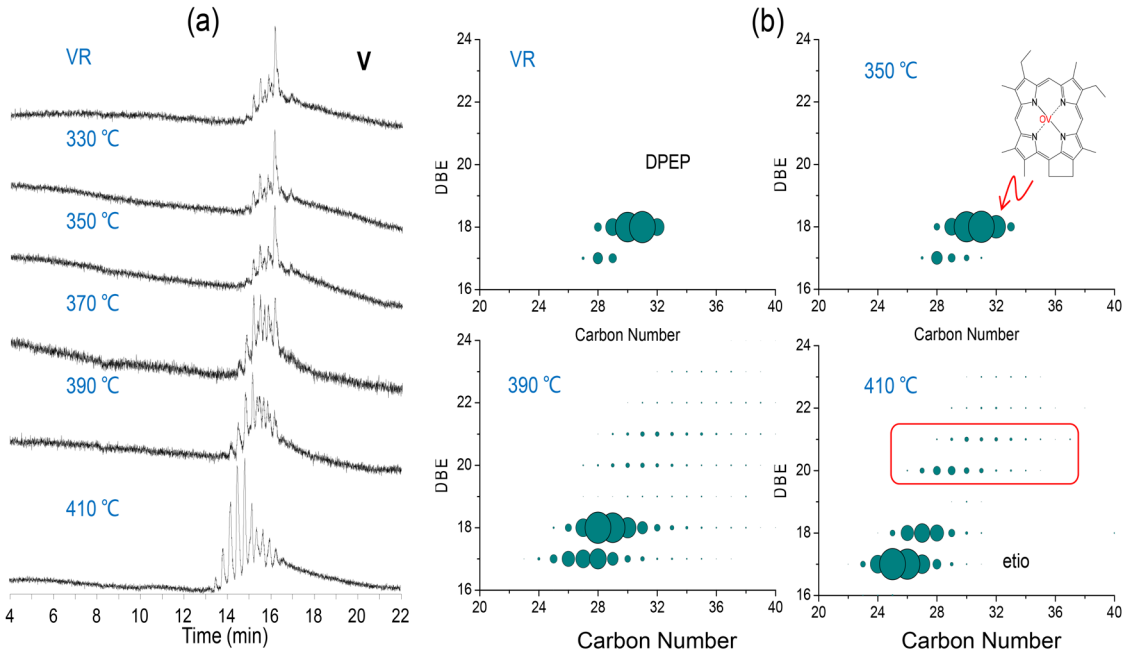

Figure 8. GC-AED (V) chromatograms (a) and DBE versus carbon number distribution of vanadyl porphyrins assigned from +ESI FT-ICR mass spectra (b) of the Venezuelan heavy oil vacuum residual and its pyrolysis products at various temperatures. Pyrolyses were conducted at 2 MP for 2 h in a hydrogen atmosphere.[158]

display both high hydrogenation and hydrogenolysis activities. Moreover, it was recently shown that demetallization can be achieved using microwave irradiation.[150] The roles of microwave and electric field irradiations were investigated through DFT calculations of vanadyl and nickel porphyrins to probe the effect of the orientation and the intensities of the sources. An electric field irradiation during the chemical treatments reduces the HOMO−LUMO gap of the metal porphyrins which may ease the metal removal.[150]

Another concern is the possibility of porphyrins to poison catalysts. Due to its closed shell character, the interaction between nickel porphyrins with the catalyst is expected to be weak unless the system is promoted in a low lying excited states.[151] On the contrary, the reactivity of vanadyl porphyrins is higher due to its radical character in the ground state of the molecule[152] or the ability to form hydrogen bonds with an acceptor through the oxygen atom. The interactions between vanadyl porphyrins and zeolite catalysts were investigated with several methodologies, ranging from static calculations[152] to quantum molecular dynamic simulations.[145] A clear affinity between zeolite surfaces and vanadyl porphyrins, associated in particular to the preferential interaction with acid or hydroxyl groups of the surface rather than water molecules, was reported.[145] Nevertheless, the adsorption itself does not cause structural damages to the zeolite. An electronic transfer was characterized from the catalyst to the metalloporphyrin, which may be the initial step leading to the degradation of the catalyst.

Joint Experimental and Theoretical Work. Collaborative works that combine experimental and theoretical methodologies are of vivid interest due to the complementary and synergistic character of the two approaches. Theoretical methodologies rely on experimental data for calibration and validation and can be predictive tools for structural, thermodynamic, or spectroscopic information.

UV−visible spectra of porphyrins were intensively investigated from a computational point of view.[124] For petroleum metal porphyrins, an accurate knowledge of optical properties is one of the commonly used probes to detect the presence of metals in crude oil. The UV−visible spectra of vanadyl and nickel porphyrins were investigated through DFT and time-dependent DFT calculations, including implicit solvation models.[69,137] The effect of axial coordination and annellation agreed well with experimental results and led to better knowledge of the Soret band shifts that occur for porphyrins bound to other compounds.[153]

Computational approaches are also implemented to proceed to a conformational analysis of candidate ions for the interpretation of trapped ion mobility spectrometry (IMS) experiments.[49] Starting from ions observed during TIMS-FT-ICR MS experiments, DFT calculations produce candidate structures of metal and free porphyrin ions through protonation of the nitrogen ring atoms or the oxygen atoms in vanadyl porphyrins. The analysis of the experimental results is then proceeded using theoretical mobility values computed from a hard sphere scattering model. Although a higher accuracy of computed mobility is expected to fully interpret the results in the case of a high resolution IMS experiment, the methodology shows its capacity to suggest ions candidates in agreement with measured mobility.

TRANSFORMATIONS OF PORPHYRINS IN HEAVY OIL PROCESSING

Thermal cracking and catalytic cracking are two main processes that convert large hydrocarbon molecules into smaller fragments and are applied to heavy oil to produce vehicle fuels and petrochemical feedstocks from low-ranked and poor-quality hydrocarbons.[154−157] The transformation of nickel and vanadium compounds in thermal cracking was rarely of concern by the petroleum industry because these metals remain in coke and did not affect the process or

https://doi.org/10.1021/acs.energyfuels.1c02002
Energy Fuels XXXX, XXX, XXX−XXX

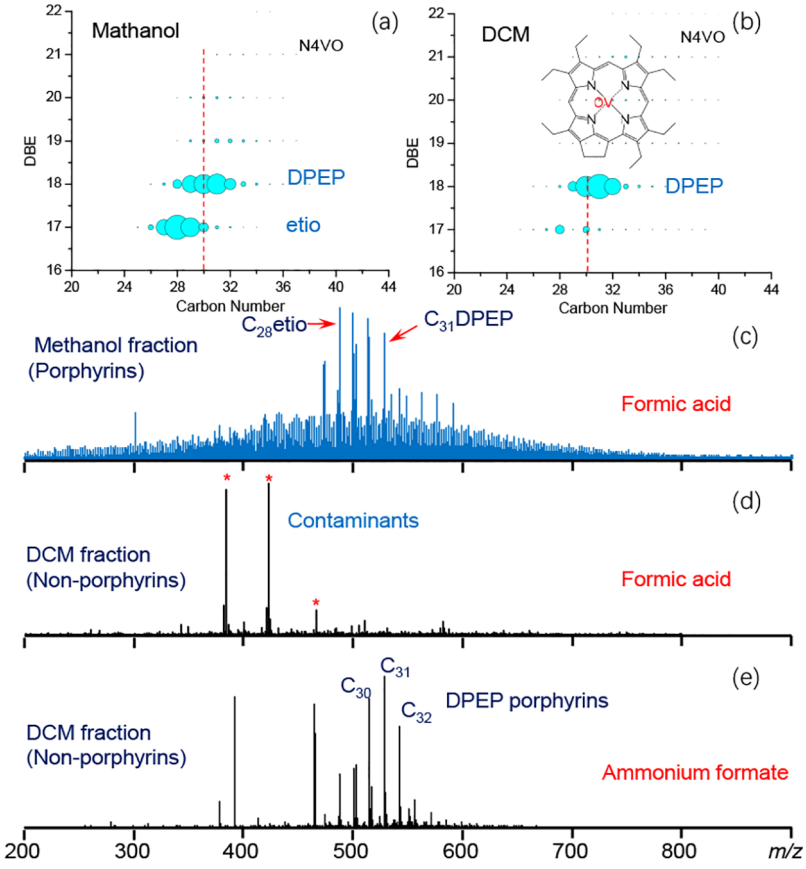

Figure 9. Porphyrins detected in the Venezuelan heavy oil fractions by +ESI FT-ICR MS. Vanadyl porphyrins assigned from the mass spectra of the porphyrin fraction (a) and nonporphyrin fraction (b). +ESI FT-ICR mass spectra of the porphyrin fraction (c) and nonporphyrin fraction (d) with formic acid and nonporphyrin fraction with ammonium formate as ionization promoter (e). Venezuelan heavy oil was loaded on diatomite and extracted by hexane, methanol, and dichloromethane (DCM) in sequence. Porphyrins and nonporphyrins were enriched in methanol and DCM fractions, respectively.[174,177]

contribute to product quality. Zheng[158] investigated the compositional changes of porphyrins in the hydropyrolysis of a Venezuelan heavy oil residue by GC-AED and ESI FT-ICR MS, which indicate side-chain breaking and aromatization occur simultaneously at high temperature (Figure 8).

Fluid Catalytic Cracking. Fluid catalytic cracking (FCC) is one of the most important processes applied worldwide to upgrade heavy petroleum fractions by converting them into lighter distillate products.[159,160] Porphyrins were of a major concern for FCC in the early days of petroleum refining mainly due to the challenges caused by nickel and vanadium compounds in heavy oils.[161] Nickel and vanadium atoms present in small organic compounds cannot transfer into lighter fractions; therefore, the only destination for Ni and V compounds is forming coke on the catalyst, which leads to metal deposition, catalyst deactivation, and coke promotion during FCC processes.[60,162] The most challenging is that the presence of vanadoxic acid produced by vanadium compounds destroys the catalyst skeleton, so to protect the catalyst and ensure normal FCC process operation, the content of Ni/V in raw FCC feeds to less than 100 ppm for vanadium, important as heavy oils that contain high V/Ni increased in production over the past decade. Importantly, low V/Ni content means lower operation cost and higher product quality, so demetallization via hydrotreating has been widely adopted for heavy oil processing.[163−167]

Hydrodemetallization. Different from FCC, the transformation mechanism of nickel and vanadium compounds is very important for the catalyst design and the optimization of process conditions in hydrogenation processes. Many studies have been carried out for the hydrodemetallization mechanism with model compounds and real samples. It was proposed that the porphyrins were converted into hydrogenated species before the demetalation; however, experimental evidences were not direct because the intermediates are not easy to characterize by traditional technologies. Recently, FT-ICR MS was used for the characterization of hydrotreated intermediates of nickel[149] and vanadyl[60] porphyrins with model compounds octaethylporphyrin (OEP). Dihydrogenated and tetrahydrogenated porphyrins were clearly detected in the ESI mass spectra, and their contents were quantified in the products obtained with oxidic and sulfided $NiMo/Al_2O_3$ catalysts, respectively. The structure of Ni-OEPH2 was speculated as 1,2-dihydro-Ni-OEPH2, which could be further hydrogenated into Ni-OEPH4. The tetrahydrogenated species is more unstable and could be easily demetallized.[149] The main pathway of Ni/V-OEP conversion during hydrotreating was the hydrodemetallization route, and Ni was removed with the porphyrin ring rapid fragmentation. It was found that VO tetrahydrogenated porphyrins are more unstable than their Ni counterpart, which could decompose at room temperature.[60,162] In addition, polar porphyrins are more prone to hydrogenation than nonpolar porphyrins.[60]

https://doi.org/10.1021/acs.energyfuels.1c02002
Energy Fuels XXXX, XXX, XXX−XXX

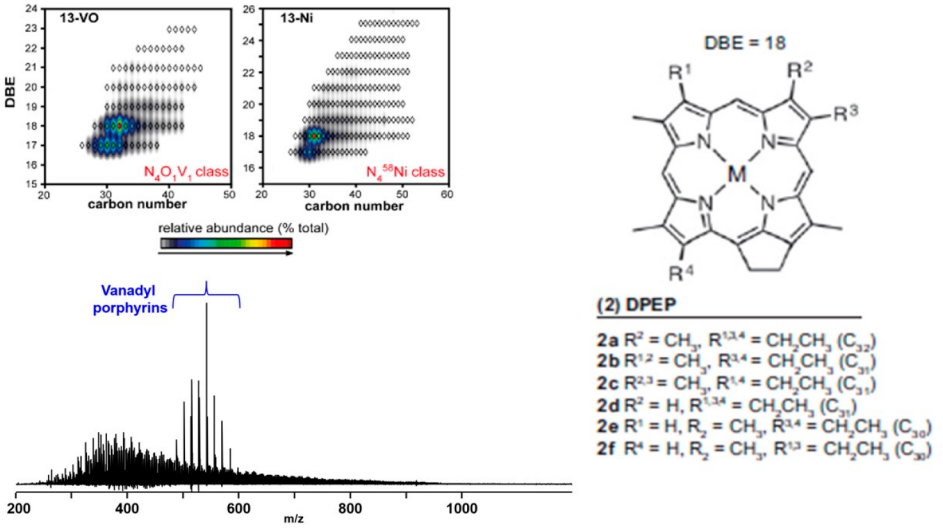

Figure 10. (Bottom left) Broadband positive-ion atmospheric pressure photoionization (APPI) 9.4 T FT-ICR mass spectrum from a Mesoproterozoic shale extract from the Taoudeni Basin that detects more than 66,000 unique elemental compositions across a molecular weight range from m/z 200−1200 with achieved mass resolving power (m/Δm50%) of 1,200,000 at m/z 500. (Top left) Identification of two classes of Ni- and VO-porphyrins by FT-ICR MS, plotting relative abundance versus double-bond equivalents (DBEs) and carbon number. (Right) Structure of C_{30} to C_{32} DPEP, one of the many porphyrin structures identified, supports phototrophs as dominant photosynthesizing organisms on Earth 1.1 billion years ago. Identified porphyrins likely derived from oxygenic phototrophs and anoxygenic phototrophic bacteria.[195]

Challenges and Limitations of MS for nonporphyrin characterization. There is always a challenge in the characterization of petroleum porphyrins: the compositions and structures of nonporphyrins. A nonporphyrin is defined as a nickel or vanadium compound without discernible visible absorption spectrum in UV−vis analysis and is nonvolatile.[28] Nonporphyrins generally account for more than ∼50% in elemental content of Ni/V, although these compounds also cannot be characterized directly by MS. Despite decades of controversy, the presence of vanadyl and nickel nonporphyrin compounds have been speculated for years.[168−170]

Yen and co-workers proposed nonporphyrins as coordination compounds, in which multiheteroatoms are coordinated with the nickel and vanadium atoms.[171−173] However, this assumption has never been proved by molecular compositional evidence. Zhao and co-workers tried to provide mass spectral evidence of nonporphyrins since FT-ICR MS was found capable of the characterization of petroleum porphyrins.[35,36] The authors identified a series of porphyrins with additional oxygen function groups. In subsequent studies, more and more nonporphyrin fractions were found containing nickel and vanadium atoms with porphyrin core structures, and substituent groups could change the optical and spectral behaviors from those of typical porphyrin complexes.

Wu et al.[174] added NH_4COOH into a nonporphyrin-enriched fraction of Venezuela heavy oil and analyzed it by +ESI MS; strong MS signals from VO compounds were detected in the FT-ICR mass spectrum (Figure 9).[174] These compounds have porphyrin composition and similar distribution with the porphyrin fraction. The results imply that nonporphyrins in the Venezuela heavy oil at least part of them are aggregates of porphyrins with other molecules. NH_4COOH destroyed the aggregation and released free porphyrins.[174]

Moulian et al.[175] investigated the effect of silver ions on the interaction between vanadium and asphaltene nanoaggregates by gel permeation chromatography inductively coupled plasma high-resolution mass spectrometry (GPC ICP-HR-MS). The results showed that disaggregation of some vanadium compounds occurred when silver ions were added.[175] In other words, the presence of silver ions changed the nonporphyrins and led to an increase in the free porphyrins.

Zheng et al.[176] characterized vanadyl porphyrins in the heavy crude oil by ion mobility spectrometry. A series of mobiligram peaks cluster ions were found in the extracted ion mobility spectra of the porphyrins, which may contain an amine in the ions. Experimental results of model compounds indicate that all the porphyrins tend to form adduct ions in the electrospray ionization, such as [2 M]+, [2 M+H]+, [2 M +Na]+, and cluster ions of porphyrin with other compounds. This implies the strong molecular aggregation potential of porphyrins with themselves and other petroleum molecules. The results are instructive for understanding of the structure of nonporphyrins, although much remains unknown.[176]

APPLICATION OF PORPHYRIN BIOMARKERS FOR GEOCHEMICAL APPLICATIONS

Porphyrins are the molecular fossils of bacteriochlorophylls, and as such, the nitrogen composition provides quantitative information about the dominant phototrophs in past ecosystems.[18,178180] Early studies more than three decades ago resulted in an upsurge in geoporphyrin research that report DPEP to Etio porphyrin ratios as maturity indicators; specifically, structural alteration of porphyrins with increased catagenesis with petroleum maturation occurs through (a) dealkylation of alkyl side chains (thus shifting to a lower carbon number across a homologous series) and (b) gradual change from DPEP to Etio as the dominant structure.[1,4,5,168,179,181] In addition, sedimentary porphyrins to trace biogeochemical processes related to past photoautotrophic activity have been widely applied to organic-rich sediments, shales, and petroleum, since structural characteristics of porphyrins reflect the source chloropigment precursors and diagenetic transformation.[1,181,182−189] In addition, stable isotopic compositions of nitrogen and carbon in geoporphyrins

https://doi.org/10.1021/acs.energyfuels.1c02002
Energy Fuels XXXX, XXX, XXX−XXX

provide critical information on source organisms.[136,144,187,190−194]

A few recent applications of porphyrin molecular composition for biogeochemical processes are highlighted below. On the basis of FT-ICR MS, petroporphyrins were identified in 1.1-billion-year old marine sedimentary rocks, and authors conclude that the ocean was dominated by cyanobacteria.[195] Molecular characterization of intact porphyrins (the molecular fossils of chlorophylls) were measured from 1.1 billion-year-old marine black shales of the Taoudeni Basin (Mauritania), 600 million years older than previous findings (Figure 10).[195]

Grosjean et al.[196] investigated weathering effects on organic matter composition from the surface to 10 m in the Paris Basin and reported the severe degradation of nickel and vanadyl porphyrins at the surface by substantial modification of their composition with preferential degradation of porphyrins with exocyclic rings over polyalkylporphyrins through weathering.[196] Compared to laboratory oxidation experiments, the authors conclude that abiotic oxidation is the predominant mechanism responsible for sedimentary porphyrin alteration.[196] Vanadyl porphyrins fractionated from a gilsonite with a high vanadium content (up to 3888 μg/g) from the Sichuan province, and China reported a large number of DPEP porphyrins, which indicated a high molecular condensation but low thermal maturity, which are important for efficient utilization of this natural source.[197] A method to quantitate Cu, Ni, VO, Zn, and Mn porphyrins in geological samples was reported by Woltering et al.,[58] who identified a range of additional compounds such as an iso-butyl C_{34} VO porphyrin indicative of paleoenvironmental photic zone euxinia and several Cu and Zn porphyrins. This method combines HPLC coupled to an Orbitrap mass spectrometer, which allows simultaneous quantitative analysis of a wide range of metalloporphyrins without the need for demetalation or fractionation.[58]

CONCLUSIONS

Targeted analysis of petroporphyrins in crude oils is possible employing selective ionization strategies such as ET MALDI. Controlling the matrix IE is fundamental to guide the analyte's ionization step and to prevent the ionization of molecules in the sample with IE higher than the matrix. As expected, metallo-porphyrin separation and isolation in samples of adequate purity requires long and tedious protocols, a feature that appears to be consequence of the relatively high amounts of porphyrins trapped within asphaltene noncovalent aggregates. ET-MALDI results in fewer interfering signals and improved analytical figures of merit. Computational approaches including both quantum mechanics calculations and molecular dynamics simulations were implemented to investigate the behavior or the intrinsic properties of petroporphyrins. The results help to elucidate the role of these specific compounds in a synergetic way with experimental data, allowing researchers to shed light on nonreachable information experimentally. Such a multitechniques approach might be pursued and encouraged in order to go further in the characterization of these compounds and the accuracy of the interpretation. Although substantial advancements in the characterization of porphyrins in geochemical systems have been facilitated by chemical information provided by advanced analytical techniques such as FT-ICR mass spectrometry, much remains for future researchers to investigate in the role of porphyrins in asphaltene aggregation and the detection and characterization of nonporphyritic species. We present this review in special recognition of Alan G. Marshall and his research collaborators over the years, who have enabled molecular characterization of these compounds at unprecedented detail.

AUTHOR INFORMATION

Corresponding Author

Amy M. McKenna − *National High Magnetic Field Laboratory, Florida State University, Tallahassee, Florida 32310-4005, United States; Department of Soil and Crop Sciences, Colorado State University, Fort Collins, Colorado 80523, USA;* orcid.org/0000-0001-7213-521X; Phone: +1 850 644 4809; Email: mckenna@magnet.fsu.edu; Fax: +1 850 644 1366

Authors

Martha L. Chacón-Patiño − *International Joint Laboratory C2MC, Complex Matrices Molecular Characterization, Total Research & Technology, BP 27, F-76700 Harfleur, France;* orcid.org/0000-0002-7273-5343

Germain Salvato Vallverdu − *Universite de Pau et des Pays de l'Adour, E2S UPPA, CNRS, IPREM, UMR5254, Pau, France; International Joint Laboratory C2MC, Complex Matrices Molecular Characterization, Total Research & Technology, BP 27, F-76700 Harfleur, France;* orcid.org/0000-0003-1116-8776

Brice Bouyssiere − *Universite de Pau et des Pays de l'Adour, E2S UPPA, CNRS, IPREM, UMR5254, Pau, France; International Joint Laboratory C2MC, Complex Matrices Molecular Characterization, Total Research & Technology, BP 27, F-76700 Harfleur, France;* orcid.org/0000-0001-5878-6067

Pierre Giusti − *Universite de Pau et des Pays de l'Adour, E2S UPPA, CNRS, IPREM, UMR5254, Pau, France; Total Research & Technology, BP 27, F-76700 Harfleur, France; International Joint Laboratory C2MC, Complex Matrices Molecular Characterization, Total Research & Technology, BP 27, F-76700 Harfleur, France; Normandie Université, COBRA, UMR 6014 et FR 3038, Université de Rouen, Mont Saint Aignan Cedex, France;* orcid.org/0000-0002-9569-3158

Carlos Afonso − *International Joint Laboratory C2MC, Complex Matrices Molecular Characterization, Total Research & Technology, BP 27, F-76700 Harfleur, France; Normandie Université, COBRA, UMR 6014 et FR 3038, Université de Rouen, Mont Saint Aignan Cedex, France;* orcid.org/0000-0002-2406-5664

Quan Shi − *State Key Laboratory of Heavy Oil Processing, China University of Petroleum, Beijing 102249, China;* orcid.org/0000-0002-1363-1237

Marianny Y. Combariza − *Escuela de Química, Universidad Industrial de Santander, Bucaramanga 680002, Colombia;* orcid.org/0000-0002-6907-4759

Complete contact information is available at: https://pubs.acs.org/10.1021/acs.energyfuels.1c02002

Notes

The authors declare no competing financial interest.

Biographies

Dr. Amy M. McKenna is an analytical environmental and petroleum chemist and Research Faculty III at the Ion Cyclotron Resonance user

https://doi.org/10.1021/acs.energyfuels.1c02002
Energy Fuels XXXX, XXX, XXX−XXX

facility at the National High Magnetic Field Laboratory, an NSF-funded laboratory at Florida State University. Since 2005, her research has focused on analytical method development for complex organic mixtures, such as petroleum, asphaltenes, weathered oil, and natural organic matter that utilize FT-ICR mass spectrometry.

Dr. Martha L. Chacón-Patiño is an expert in analytical chemistry, with a focus on the characterization of complex organic mixtures by separations and ultrahigh-resolution mass spectrometry. In the last 10 years, she has explored the molecular composition of one of the most complex organic mixtures, the asphaltenes, and their role as precursors of emerging/water-soluble contaminants in the built environment.

Dr. Germain Salvato Vallverdu obtained his Ph.D. (2009) in chemical physics from the University Paris−Saclay. Since 2010, he has been an associate professor at the Université de Pau et des Pays de l'Adour and a specialist in theoretical chemistry and molecular simulations. For the last 10 years, he has been working on the development of computational strategies in close collaboration with experimental techniques and considered materials for energy storage and molecular characterization of complex matrices.

Prof. Brice Bouyssiere is a Professor of analytical chemistry at the University of Pau and one of the responsible and the co-founder of the International Lab on Complex Matrices Molecular Characterization (iC2MC lab). After Chemical and Process Engineering School (ENSGTI) and a Ph.D. dealing with speciation of mercury and arsenic in gas condensates at the University of in Pau, he did a postdoctoral stay at the GKSS Geesthacht, Germany. His principal research interest is metals speciation in complex matrices.

Dr. Pierre Giusti obtained his Ph.D. in analytical chemistry from the University of Pau and Pays de l'Adour in 2006. He is currently the manager of the Molecular Separation and Identification Service in the R&D department of TotalEnergies Refining & Chemicals. He is the co-founder of the iC2MC laboratory, and he also obtained the position of CNRS Research Director in January 2021. His research interests are the elemental and molecular analyses of complex matrices in the field of energy.

Prof. Carlos Afonso currently works at the Chimie Organique et Bioorganique: Réactivité et Analyse lab (COBRA), Université de Rouen. He does research in analytical chemistry and spectroscopy. The Rouen MS group is focused on the analysis of biological and chemical highly complex mixtures based on Fourier transform mass spectrometry and ion mobility-mass spectrometry.

Prof. Quan Shi is a professor at the China University of Petroleum (Beijing) and a Deputy Director at the China State Key Laboratory of Heavy Oil Processing. Dr. Shi specializes in analytical chemistry and petroleomics. He holds BS and MS degrees in chemical engineering from the China University of Petroleum and a Ph.D. in geological chemistry from the China University of Geology.

Prof. Marianny Y. Combariza works at the School of Chemistry, Universidad Industrial de Santander, Colombia. Her work focuses on complex mixture analysis using HRMS, selective ionization, and labile compound analysis by MALDI MS, biosynthesis, isolation, characterization, and modification of biopolymers from residual lignocellulosic biomass.

■ ACKNOWLEDGMENTS

This work was supported by the NSF Division of Chemistry and Division of Materials Research through DMR-1644779 and the State of Florida. M.Y.C. acknowledges the Guatiguará Technology Park and the Mass Spectrometry Lab−Central Research Laboratory Facility at Universidad Industrial de Santander for infrastructural assistance and the Colombian Ministry of Science, Technology, and Innovation for financial support. Q.S. was supported by the National Science Foundation of China through NSFC U19B2002. C.A. acknowledges financial support from the CNRS FTICR research infrastructure (FR3624), European Union's Horizon 2020 Research Infrastructures program (Grant Acknowledgement 731077), and Laboratoire d'Excellence (LabEx) SynOrg (ANR-11-LABX-0029).

■ REFERENCES

(1) Baker, E. W.; Louda, J. W.; Orr, W. L. Application of metalloporphyrin biomarkers as petroleum maturity indicators: The importance of quantitation. *Org. Geochem.* **1987**, *11* (4), 303−309.
(2) Biesaga, M.; Pyrzynska, K.; Trojanowicz, M. Porphyrins in analytical chemistry. A review. *Talanta* **2000**, *51* (2), 209−224.
(3) Milgrom, L. R. *The Coulours of Life: An Introduction to the Chemistry of Porphyrins and Related Compounds*; Oxford University Press: Oxford, U.K., 1999.
(4) Baker, E. W. Mass spectrometric characterization of petroporphyrins. *J. Am. Chem. Soc.* **1966**, *88* (10), 2311−2311.
(5) Baker, E. W.; Yen, T. F.; Dickie, J. P.; Rhodes, R. E.; Clark, L. F. Mass spectrometry of porphyrins. II. Characterization of petroporphyrins. *J. Am. Chem. Soc.* **1967**, *89* (4), 3631−3639.
(6) Ali, M. F.; Abbas, S. A review of methods for the demetallization of residual fuel oils. *Fuel Process. Technol.* **2006**, *87*, 573−584.
(7) Dodds, J. N.; Baker, E. S. Ion mobility spectrometry: Fundamental concepts, instrumentation, applications and the road ahead. *J. Am. Soc. Mass Spectrom.* **2019**, *30*, 2185−2195.
(8) Treibs, A. Occurrence of chlorophyll derivatives in an oil shale of the upper Triassic. *Justus Liebigs Ann. Chem.* **1934**, *509*, 103−114.
(9) Treibs, A. Organic mineral substances. V. Porphyrins in coals. *Justus Liebigs Ann. Chem.* **1935**, *520*, 144−150.
(10) Treibs, A. Organic mineral substances. IV. Chlorophyll and hemin derivatives in bituminous rocks, petroleums, coals and phosphorites. *Justus Liebigs Ann. Chem.* **1935**, *517*, 172−196.
(11) Treibs, A. Chlorophyll and hemin derivatives in organic mineral substances. *Angew. Chem.* **1936**, *49* (38), 682−686.
(12) Dechaine, G. P.; Gray, M. R. Chemistry and association of vanadium compounds in heavy oil and bitumen, and implications for their selective removal. *Energy Fuels* **2010**, *24* (5), 2795−2808.
(13) Ramírez-Pradilla, J. S.; Blanco-Tirado, C.; Hubert-Roux, M.; Giusti, P.; Afonso, C.; Combariza, M. Y. Comprehensive Petroporphyrin Identification in Crude Oils Using Highly Selective Electron Transfer Reactions in MALDI-FTICR-MS. *Energy Fuels* **2019**, *33* (5), 3899−3907.
(14) Hodgson, G. W.; Peake, E. Metal chlorin complexes in recent sediments as initial precursors to petroleum porphyrin pigments. *Nature* **1961**, *191*, 766.
(15) Sundararaman, P. On the mechanism of change in DPEP/ETIO ratio with maturity. *Geochim. Cosmochim. Acta* **1993**, *57*, 4517−4520.
(16) Filby, R. H.; van Berkel, G. J. Geochemistry of Metal Complexes in Petroleum, Source Rocks, and Coals: An Overview. In *Metal Complexes in Fossil Fuels*; Filby, R. H., Branthaver, J. F., Eds.; ACS Symposium Series 344; American Chemical Society, Washington, DC, 1987; pp 2−39.
(17) Lash, T. D. Geochemical origins of sedimentary benzoporphyrins and tetrahydrobenzoporphyrins. *Energy Fuels* **1993**, *7*, 166−171.
(18) Thomas, D. W.; Blumer, M. Porphyrin pigments of a Triassic sediment. *Geochim. Cosmochim. Acta* **1964**, *28* (7), 1147−1154.
(19) Hajibrahim, S.K.; Quirke, J.M.E.; Eglinton, G. Petroporphyrins: V. Structurally-related porphyrin series in bitumens, shales and petroleum- Evidence from HPLC and mass spectrometry. *Chem. Geol.* **1981**, *32*, 173−188.
(20) Ekstrom, A.; Fookes, C. J. R.; Hambley, T.; Loeh, H. J.; Miller, S. A.; Taylor, J. C. Determination of the crystal structure of a

https://doi.org/10.1021/acs.energyfuels.1c02002
Energy Fuels XXXX, XXX, XXX−XXX

petroporphyrin isolated from oil shale. *Nature* **1983**, *306* (5939), 173−174.
(21) Zhang, Y.; Schulz, F.; McKay Rytting, B.; Walters, C. C.; Kaiser, K.; Metz, J. N.; Harper, M. R.; Merchant, S. S.; Mennito, A. S.; QIan, K.; Kushnerick, J. D.; Kilpatrick, P. K.; Gross, L. Elucidating the geometric substitution of petroporphyrins by spectroscopic analysis and atomic force microscopy molecular imaging. *Energy Fuels* **2019**, *33*, 6088−6097.
(22) Zheng, F.; Shi, Q.; Vallverdu, G. S.; Giusti, P.; Bouyssiere, B. Fractionation and Characterization of Petroleum Asphaltene: Focus on Metalopetroleomics. *Processes* **2020**, *8*, 1504.
(23) Mironov, N. A.; Milordov, D. V.; Abilova, G. R.; Yakubova, S. G.; Yakubov, M. R. Methods for studying petroleum porphyrins (Review). *Pet. Chem.* **2019**, *59* (10), 1077−1091.
(24) Gallegos, E. J.; Sundararaman, P. Mass spectrometry of geoporphyrins. *Mass Spectrom. Rev.* **1985**, *4*, 55−85.
(25) Rodgers, R. P.; McKenna, A. M. Petroleum analysis. *Anal. Chem.* **2011**, *83*, 4665−4687.
(26) Kim, S.; Kim, D.; Jung, M.-J.; Kim, S. Analysis of environmental organic matters by Ultrahigh-Resolution mass spectrometry—A review on the development of analytical methods. *Mass Spectrom. Rev.* **2021**, 1−18.
(27) Bonnett, R. Porphyrins in coal. *Int. J. Coal Geol.* **1996**, *32*, 137−149.
(28) Zhao, X.; Xu, C.; Shi, Q. Porphyrins in Heavy Petroleums: A Review. *Struct. Bonding (Berlin, Ger.)* **2015**, *168*, 39−70.
(29) Rodgers, R. P.; Hendrickson, C. L.; Emmett, M. R.; Marshall, A. G.; Greaney, M. A.; Qian, K. Molecular Characterization of Petroporphyrins in Crude Oil by Electrospray Ionization Fourier Transform Ion Cyclotron Resonance Mass Spectrometry. *Can. J. Chem.* **2001**, *79*, 546−551.
(30) McKenna, A. M.; Purcell, J. M.; Rodgers, R. P.; Marshall, A. G. Identification of vanadyl porphyrins in a heavy crude oil and raw asphaltene by atmospheric pressure photoionization Fourier transform ion cyclotron resonance (FT-ICR) mass spectrometry. *Energy Fuels* **2009**, *23* (4), 2122−2128.
(31) McKenna, A. M.; Williams, J. T.; Putman, J. C.; Aeppli, C.; Reddy, C. M.; Valentine, D. L.; Lemkau, K. L.; Kellermann, M. Y.; Savory, J. J.; Kaiser, N. K.; Marshall, A. G.; Rodgers, R. P. Unprecedented ultrahigh resolution FT-ICR mass spectrometry and parts-per-billion mass accuracy enable direct characterization of nickel and vanadyl porphyrins in petroleum from natural seeps. *Energy Fuels* **2014**, *28*, 2454−2464.
(32) Qian, K.; Mennito, A. S.; Edwards, K. E.; Ferrughelli, D. T. Observation of vanadyl porphyrins and sulfur-containing vanadyl porphyrins in a petroleum asphaltene by atmospheric pressure photonionization Fourier transform ion cyclotron resonance mass spectrometry. *Rapid Commun. Mass Spectrom.* **2008**, *22* (14), 2153−2160.
(33) Qian, K.; Edwards, K. E.; Mennito, A. S.; Walters, C. C.; Kushnerick, J. D. Enrichment, Resolution, and Identification of Nickel Porphyrins in Petroleum Asphaltene by Cyclograph Separation and Atmospheric Pressure Photoionization Fourier Transform Ion Cyclotron Resonance Mass Spectrometry. *Anal. Chem.* **2010**, *82* (1), 413−419.
(34) Zheng, F.; Hsu, C. S.; Zhang, Y.; Sun, Y.; Wu, Y.; Lu, H.; Sun, X.; Shi, Q. Simultaneous detection of vanadyl, nickel, iron and gallium porphyrins in marine shales from the Eagle Ford formation, South Texas. *Energy Fuels* **2018**, *32* (10), 10382−10390.
(35) Zhao, X.; Liu, Y.; Xu, C.; Yan, Y.; Zhang, Y.; Zhang, Q.; Zhao, S.; Chung, K.; Gray, M. R.; Shi, Q. Separation and characterization of vanadyl porphyrins in Venezuela Orinoco heavy crude. *Energy Fuels* **2013**, *27* (6), 2874−2882.
(36) Zhao, X.; Shi, Q.; Gray, M. R.; Xu, C. New vanadium compounds in Venezuela heavy crude oil detected by positive-ion electrospray ionization fourier transform ion cyclotron resonance mass spectrometry. *Sci. Rep.* **2015**, *4*, 5373.
(37) Qian, K.; Fredriksen, T. R.; Mennito, A. S.; Zhang, Y.; Harper, M. R.; Merchant, S.; Kushnerick, J. D.; Rytting, B. M.; Kilpatrick, P. K. Evidence of naturally-occurring vanadyl porphyrins containing multiple S and O atoms. *Fuel* **2019**, *239*, 1258−1264.
(38) Faramawy, S.; El-Sabagh, S. M.; Moustafa, Y. M.; El-Naggar, A. Y. Mass spectrometry of metalloporphyrins in Egyption oil shales from Red Sea area. *Pet. Sci. Technol.* **2010**, *28* (6), 603−617.
(39) Jarvis, J. M.; Sudasinghe, N. M.; Albrecht, K. O.; Schmidt, A. J.; Hallen, R. T.; Anderson, D. B.; Billing, J. M.; Schaub, T. M. Impact of iron porphyrin complexes when hydroprocessing algal HTL biocrude. *Fuel* **2016**, *182*, 411−418.
(40) Putman, J. C.; Rowland, S. M.; Corilo, Y. E.; McKenna, A. M. Chromatographic enrichment and subsequent separation of nickel and vanadyl porphyrins from natural seeps and molecular characterization by positive electrospray ionization FT-ICR mass spectrometry. *Anal. Chem.* **2014**, *86* (32), 10708−10715.
(41) Suwarno, A. C.; Yulizar, Y.; Haerudin, H.; Kurniawaty, I.; Apriandanu, D. O. B. Investigation of metalloporphyrin in maltenes phase of crude oil Duri. *J. Phys.: Conf. Ser.* **2020**, *1442*, 012049.
(42) McDaniel, E.; Martin, D. W.; Barnes, W. S. Drift tube-mass spectrometer for studies of low-energy ion−molecule reactions. *Rev. Sci. Instrum.* **1962**, *33* (1), 2−7.
(43) Campuzano, I.; Bush, M. F.; Robinson, C. V.; Beaumont, C.; Richardson, K.; Kim, H.; Kim, I. Structural characterization of drug-like compounds by ion mobility mass spectrometry: Comparison of theoretical and experimentally dervied nitrogen collision cross sections. *Anal. Chem.* **2012**, *84* (2), 1026−1033.
(44) Kailemia, M. J.; Park, M.; Kaplan, D. A.; Venot, A.; Boons, G. J.; Li, L.; Linhardt, R. J.; Amster, I. J. High-field asymmetric-waveform ion mobility spectrometry and electron detachment dissociation of isobaric mixtures of glycosaminoglycans. *J. Am. Soc. Mass Spectrom.* **2014**, *25* (2), 258−268.
(45) Benigni, P.; Marin, R.; Fernandez-Lima, F. A. Towards unsupervised polyaromatic hydrocarbons strucutral assignment from SA-TIMS-FTMS data. *Int. J. Ion Mobility Spectrom.* **2015**, *18* (3), 151−157.
(46) Benigni, P.; Fernandez-Lima, F. A. Oversampling Selective Accumulation Trapped Ion Mobility Spectrometry Coupled to FT-ICR MS: Fundamentals and Applications. *Anal. Chem.* **2016**, *88* (14), 7404−7412.
(47) Mason, E. A.; Schamp, H. W. Mobility of gaseous ions in weak electric fields. *Ann. Phys.* **1958**, *4* (3), 233−270.
(48) Zheng, F.; Zhang, Y.; Zhang, Y.; Han, Y.; Zhang, L.; Bouyssiere, B.; Shi, Q. Aggregation of petroporphyrins and fragmentation of porphyrin ions: Characterized by TIMS-TOF MS and FT-ICR MS. *Fuel* **2021**, *289*, 119889.
(49) Benigni, P.; Bravo, C.; Quirke, J. M. E.; DeBord, J. D.; Mebel, A. M.; Fernandez-Lima, F. A. Analysis of geologically relevant metal porphyrins using trapped ion mobility spectrometry-mass spectrometry and theoretical calculations. *Energy Fuels* **2016**, *30* (12), 10341−10347.
(50) Maillard, J. F.; Le Maître, J.; Rüger, C.; Ridgeway, M. E.; Thompson, C. J.; Paupy, B.; Hubert-Roux, M.; Park, M. A.; Afonso, C.; Giusti, P. Structural analysis of petroporphyrins from asphaltene by trapped ion mobility coupled with a Fourier transform ion cyclotron resonance mass spectrometer. *Analyst* **2021**, *146* (13), 4161−4171.
(51) Smith, D. F.; Blakney, G. T.; Beu, S. C.; Anderson, L. C.; Weisbrod, C. R.; Hendrickson, C. L. Ultrahigh resolution ion isolation by stored waveform inverse Fourier transform 21 T Fourier transform ion cyclotron resonance mass spectrometry. *Anal. Chem.* **2020**, *92* (4), 3213−3219.
(52) Beato, B. D.; Yost, R. A.; Quirke, J. M. E. Doubly charged porphyrin ion tandem mass spectrometry: Implications for structure elucidation. *Org. Mass Spectrom.* **1989**, *24* (10), 875−884.
(53) Johnson, J. V.; Britton, E. D.; Yost, R. A.; Quirke, J. M. E.; Cuesta, L. L. Tandem mass spectrometry for characterization of high-carbon number geoporphyrins. *Anal. Chem.* **1986**, *58* (7), 1325−1329.
(54) Beato, B. D.; Yost, R. A.; Quirke, J. M. E. Carbon number, pyrrolic structure and sequencing information of porphyrin structure

https://doi.org/10.1021/acs.energyfuels.1c02002
Energy Fuels XXXX, XXX, XXX−XXX

in one experiment by desorption tandem mass spectrometry—relevance for geoporphyrins. *Chem. Geol.* **1991**, *91* (2), 185−192.
(55) Laycock, J. D.; Ferguson, J. A.; Yost, R. A.; Quirke, J. M. E.; Rohrer, A.; O'Campo, R.; Callot, H. J. Electron ionization mass spectrometric analysis of 5-nitro octaethylporphyrin: Evidence for scission of the porphyrin macrocycle. *J. Mass Spectrom.* **1997**, *32* (9), 978−983.
(56) Van Berkel, G. J.; McLuckey, S. A.; Glish, G. L. Unimolecular and collision-induced reactions of doubly charged porphyrins. *J. Am. Soc. Mass Spectrom.* **1992**, *3* (3), 235−242.
(57) Rosell-Mele, A.; Carter, J. F.; Maxwell, J. R. HIgh-performance liqud chromatogrpahy-mass spectrometry of porphyrins by using an atmospheric pressure interface. *J. Am. Soc. Mass Spectrom.* **1996**, *7*, 965−971.
(58) Woltering, M.; Tulipani, S.; Boreham, C. J.; Walshe, J.; Schwark, L.; Grice, K. Simultaneous quantitative analysis of Ni, VO, Cu, Zn and Mn geoporphyrins by liquid chromatography-high resolution multistage mass spectrometry: Method development and validation. *Chem. Geol.* **2016**, *441*, 81−91.
(59) Xu, H.; Que, G.; Yu, D.; Lu, J. R. Characterization of petroporphyrins using ultraviolet-visibile spectroscopy and laser desorption ionization time-of-flight mass spectrometry. *Energy Fuels* **2005**, *19* (2), 517−524.
(60) Liu, H.; Mu, J.; Wang, Z.; Ji, S.; Shi, Q.; Guo, A.; Chen, K.; Lu, J. Characterization of vanadyl and nickel porphyrins enriched from heavy residues by positive-ion electrospray ionization FT-ICR mass spectrometry. *Energy Fuels* **2015**, *29*, 4803−4813.
(61) McLafferty, F. W.; Turecek, F. *Interpretation of Mass Spectra*, 4th ed.; University Science Books: Mill Valley, CA, 1993.
(62) Liu, T.; Lu, J.; Zhao, X.; Zhou, Y.; Wei, Q.; Xu, C.; Zhang, Y.; Ding, S.; Zhang, T.; Tao, X.; Ju, L.; Shi, Q. Distribution of vanadium compounds in petroleum vacuum residuum and their transformationsin hydrodemetallization. *Energy Fuels* **2015**, *29* (4), 2089−2096.
(63) Chauhan, G.; de Klerk, A. Acidified ionic liquid assisted recovery of vanadium and nickel from oilsands bitumen. *Energy Fuels* **2021**, *35* (7), 5963−5974.
(64) Gascon, G.; Negrin, J.; Garcia-Montoto, V.; Acevedo, S.; Lienemann, C. P.; Bouyssiere, B. Simplification of heavy matrices by liquid-liquid extraction: Part 1- How to separate LMW, MMW, and HMW compounds in maltene fractions of V, Ni, and S compounds. *Energy Fuels* **2019**, *33* (3), 1922−1927.
(65) Zhang, Y.; Zhang, L.; Xu, Z.; Zhang, N.; Chung, K. H.; Zhao, S.; Xu, C.; Shi, Q. Molecular characterization of vacuum resid and its fractions by Fourier transform ion cyclotron resonance mass spectrometry with various ionization techniques. *Energy Fuels* **2014**, *28* (12), 7448−7456.
(66) Yin, C.-X.; Stryker, J. M.; Gray, M. R. Separation of petroporphyrins from asphaltenes by chemical modification and selective affinity chromatography. *Energy Fuels* **2009**, *23*, 2600−2605.
(67) Yin, C.-X.; Stryker, J. M.; Gray, M. R. Separation of petroporphyrins from asphaltenes by chemical modification and selective affinity chromatography. *Energy Fuels* **2009**, *23* (5), 2600−2605.
(68) Acevedo, S.; Guzman, K.; Labrador, H.; Carrier, H.; Bouyssiere, B.; Lobinski, R. Trapping of Metallic Porphyrins by Asphaltene Aggregates: A Size Exclusion Microchromatography With High-Resolution Inductively Coupled Plasma Mass Spectrometric Detection Study. *Energy Fuels* **2012**, *26* (8), 4968−4977.
(69) Stoyanov, S. R.; Yin, C.-X.; Gray, M. R.; Stryker, J. M.; Gusarov, S.; Kovalenko, A. Computational and experimental study of the structure, binding preferences, and spectroscopy of nickel(II) and vanadyl porphyrins in petroleum. *J. Phys. Chem. B* **2010**, *114* (6), 2180−2188.
(70) Desprez, A.; Bouyssiere, B.; Arnaudguilhem, C.; Krier, G.; Vernex-Loset, L.; Giusti, P. Study of the Size Distribution of Sulfur, Vanadium, and Nickel Compounds in Four Crude Oils and Their Distillation Cuts by Gel Permeation Chromatography Inductively Coupled Plasma High-Resolution Mass Spectrometry. *Energy Fuels* **2014**, *28* (6), 3730−3737.
(71) Gascon, G.; Vargas, V.; Feo, L.; Castellano, O.; Castillo, J.; Giusti, P.; Acavedo, S.; Lienemann, C. P.; Bouyssiere, B. Size distributions of sulfur. vanadium, and nickel compounds in crude oils, residues, and their saturate, aromatic, resin, and asphaltene fractions determined by gel permeation chromatography inductively coupled plasma high-resolution mass spectrometry. *Energy Fuels* **2017**, *31* (8), 7783−7788.
(72) Putman, J. C.; Moulian, R.; Barrère-Mangote, C.; Rodgers, R. P.; Bouyssiere, B.; Giusti, P.; Marshall, A. G. Probing Aggregation Tendencies in Asphaltenes by Gel Permeation Chromatography. Part 1: Online Inductively Coupled Plasma Mass Spectrometry and Offline Fourier Transform Ion Cyclotron Resonance Mass Spectrometry. *Energy Fuels* **2020**, *34* (7), 8308−8315.
(73) Hsu, C. S.; Lobodin, V. V.; Rodgers, R. P.; McKenna, A. M.; Marshall, A. G. Compositional boundaries for fossil hydrocarbons. *Energy Fuels* **2011**, *25* (5), 2174−2178.
(74) Putman, J. C.; Moulian, R.; Smith, D. F.; Weisbrod, C. R.; Chacón-Patiño, M. L.; Corilo, Y. E.; Blakney, G. T.; Rumancik, L. E.; Barrère-Mangote, C.; Rodgers, R. P.; Giusti, P.; Marshall, A. G.; Bouyssière, B. Probing Aggregation Tendencies in Asphaltenes by Gel Permeation Chromatography. Part 2: Online Detection by Fourier Transform Ion Cyclotron Resonance Mass Spectrometry and Inductively Coupled Plasma Mass Spectrometry. *Energy Fuels* **2020**, *34* (9), 10915−10925.
(75) Altgelt, K. H. Fractionation of asphaltenes by gel permeation chromatography. *J. Appl. Polym. Sci.* **1965**, *9*, 3389−3393.
(76) Coleman, H. J.; Hirsch, D. E.; Dooley, J. E. Separation of crude oil fractions by gel permeation chromatography. *Anal. Chem.* **1969**, *41* (6), 800−804.
(77) Sato, S.; Takanohashi, T.; Tanaka, R. Molecular weight calibration using gel permeation chromatography/mass spectrometry. *Energy Fuels* **2005**, *19* (5), 1991−1994.
(78) Sato, S.; Takanohashi, T.; Tanaka, R. Molecular weight calibration of asphaltenes using gel permeation chromatography/mass spectrometry. *Energy Fuels* **2005**, *19* (5), 1991−1994.
(79) Putman, J. C.; Chacón-Patiño, M. L.; Rowland, S. M.; Weisbrod, C. R.; Smith, D. F.; Corilo, Y. E.; Barrer-Mangote, C.; Bouyssiere, B.; Giusti, P.; Rodgers, R. P.; Marshall, A. G. Chromatography/Fourier Transform Ion Cyclotron Resonance Mass Spectrometry: Probing Aggregation Tendencies in Asphaltenes and Petroleum Products; 19th International Conference on Petroleum Phase Behavior and Fouling, PetroPhase; Salt Lake City, Utah, July 8−12, 2018.
(80) Garcia-Montoto, V.; Verdier, S.; Maroun, Z.; Egeberg, R.; Tiedje, J. L.; Sandersen, S.; Zeuthen, P.; Bouyssiere, B. Understanding the removal of V, Ni and S in crude oil atmospheric residue hydrodemtallization and hydrodesulfurization. *Fuel Process. Technol.* **2020**, *201*, 106341.
(81) Moulian, R.; Chacón-Patiño, M. L.; Lacroix-Andrivet, O.; Mounicou, S.; Mendes Siqueira, A. L.; Afonso, C.; Rodgers, R. P.; Giust, P.; Bouyssiere, B.; Barrère-Mangote, C. Speciation of Metals in Asphaltenes by High-Performance Thin-Layer Chromatography and Solid−Liquid Extraction Hyphenated with Elemental and Molecular Identification. *Energy Fuels* **2020**, *34* (10), 12449−12456.
(82) Yin, C.-X.; Tan, X.; Mullen, K.; Stryker, J. M.; Gray, M. R. Associative $\pi-\pi$ Interactions of condensed aromatic compounds with vanadyl or nickel porphyrin complexes are not observed in the organic phase. *Energy Fuels* **2008**, *22* (4), 2465−2469.
(83) Chacón-Patiño, M. L.; Rowland, S. M.; Rodgers, R. P. Advances in asphaltene petroleomics. Part 2: A selective separation method that reveals fractions enriched in island and archipelago strucutral motifs by mass spectrometry. *Energy Fuels* **2018**, *32* (1), 314−328.
(84) Chacón-Patiño, M. L.; Rowland, S. M.; Rodgers, R. P. Advances in Asphaltene Petroleomics. Part 3. Dominance of island or archipelago structural motif is sample dependent. *Energy Fuels* **2018**, *32* (9), 9106−9120.

https://doi.org/10.1021/acs.energyfuels.1c02002
Energy Fuels XXXX, XXX, XXX−XXX

(85) Chacón-Patiño, M. L.; Smith, D. F.; Hendrickson, C. L.; Marshall, A. G.; Rodgers, R. P. Advances in Asphaltene Petroleomics. Part 4. Compositional Trends of Solubility Subfractions Reveal that Polyfunctional Oxygen-Containing Compounds Drive Asphaltene Chemistry. *Energy Fuels* **2020**, *34* (3), 3013−3030.
(86) Castellanos-Garcia, L. J.; Agudelo, B. C.; Rosales, H. F.; Cely, M.; Ochoa-Puentes, C.; Blanco-Tirado, C.; Sierra, C. A.; Combariza, M. Y. Oligo p-Phenylenevinylene Derivatives as Electron Transfer Matrices for UV-MALDI. *J. Am. Soc. Mass Spectrom.* **2017**, *28*, 2548−2560.
(87) Giraldo-Dávila, D.; Chacón-Patiño, M. L.; Ramirez-Pradillia, J. S.; Blanco-Tirado, C.; Combariza, M. Y. Selective ionization by electron-transfer MALDI-MS of vanadyl porphyrins from crude oils. *Fuel* **2018**, *226*, 103−111.
(88) Evdokimov, I. N.; Fesan, A. A.; Losev, A. P. Occlusion of foreign molecules in primary asphaltene aggregates from near-UV-Visible absorption studies. *Energy Fuels* **2017**, *31* (2), 1370−1375.
(89) Pereira, S. F. J.; Moraes, D. P.; Antes, F. G.; Diehl, L. O.; Santos, M. F. P.; Guimarães, R. C. L.; Fonseca, T. C. O.; Dressler, V. L.; Flores, E. M. M. Determination of metals and metalloids in light and heavy crude oil by ICP-MS after digestion by microwave-induced combustion. *Microchem. J.* **2010**, *96*, 4−11.
(90) Fan, S.; Liu, H.; Wang, J.; Chen, H.; Bai, R.; Guo, A.; Chen, K.; Huang, J.; Wang, Z. Microwave-assisted Petroporphyrin Release from Asphaltene Aggregates in Polar Solvents. *Energy Fuels* **2020**, *34* (3), 2683−2692.
(91) Bjorndalen, N.; Islam, M. R. The effect of microwave and ultrasonic irradiation on crude oil during production with a horizontal well. *J. Pet. Sci. Eng.* **2004**, *43*, 139−150.
(92) Xia, L.; Lu, S.; Cao, G. Stability and demulsifcation of emulsions stabilized by asphaltenes or resins. *J. Colloid Interface Sci.* **2004**, *271*, 504−506.
(93) Kelemen, S. R.; Afeworki, M.; Gorbaty, M. L.; Sansone, M.; Kwiatek, P. J.; Walters, C. C.; Freund, H.; Siskin, M.; Bence, A. E.; Curry, D. J.; Solum, M.; Pugmire, R. J.; Vandenbroucke, M.; Leblond, M.; Behar, F. Direct characterization of kerogen by X-ray and Solid-State 13C Nuclear Magnetic Resonance methods. *Energy Fuels* **2007**, *21* (3), 1548−1561.
(94) Siskin, M.; Kelemen, S. R.; Eppig, C. P.; Brown, L. D.; Afeworki, M. Asphaltene molecular structure and chemical influences on the morphology of coke produced in delayed coking. *Energy Fuels* **2006**, *20* (3), 1227−1234.
(95) Rytting, B. M.; Singh, I. D.; Kilpatrick, P. K.; Harper, M. R.; Mennito, A. S.; Zhang, Y. Ultrahigh-purity vanadyl petroporphyrins. *Energy Fuels* **2018**, *32* (5), 5711−5724.
(96) Rytting, B. M.; Harper, M. R.; Edmond, K. V.; Zhang, Y.; Kilpatrick, P. K. High-purity vanadyl petroporphyrins: Their aggregation and effect on the aggregation of asphaltenes. *Energy Fuels* **2020**, *34* (1), 164−178.
(97) Rytting, B. M.; Harper, M. R.; Edmond, K. V.; Merchant, S.; Zhang, Y.; Kilpatrick, P. K. Interfacial phenomena of purified petroporphyrins and their impact on asphaltene interfacial film formation. *Energy Fuels* **2020**, *34* (5), 5444−5456.
(98) Mironov, N. A.; Milordov, D. V.; Tazeeva, E. G.; Abilova, G. R.; Tazeev, D. I.; Morozov, V. I.; Yakubova, S. G.; Yakubov, M. R. Influence of the composition of the sulfuric acid cation exchanger on the efficiency of chromatographic purification of petroleum vanadyl porphyrins. *Russ. J. Appl. Chem.* **2020**, *93*, 888−896.
(99) Mironov, N. A.; Abilova, G. R.; Sinyashin, K. O.; Gryaznov, P. I.; Borisova, Y. Y.; Milordov, D. V.; Tazeeva, E. G.; Yakubova, S. G.; Borisov, D. N.; Yakubov, M. R. Chromatographic isolation of petroleum vanadyl porphyrins using sulfocationites as sorbents. *Energy Fuels* **2018**, *32*, 161−168.
(100) Mironov, N. A.; Abilova, G. R.; Borisova, Y. Y.; Tazeeva, E. G.; Milordov, D. V.; Yakubova, S. G.; Yakubov, M. R. Comparative Study of Resins and Asphaltenes of Heavy Oils as Sources for Obtaining Pure Vanadyl Porphyrins by the Sulfocationite-Based Chromatographic Method. *Energy Fuels* **2018**, *32* (12), 12435−12446.
(101) Grigsby, R. D.; Green, J. B. High-resolution mass spectrometric analysis of a vanadyl porphyrin fraction isolated from the > 700 C resid of Cerro Negro heavy petroleum. *Energy Fuels* **1997**, *11* (3), 602−609.
(102) Rodgers, R. P.; Marshall, A. G. Petroleomics: Advanced Characterization of Petroleum-Derived Materials Characterized by Fourier Transform Ion Cyclotron Resonance Mass Spectrometry (FT-ICR MS). In *Asphaltenes, Heavy Oils and Petroleomics*; Mullins, O. C., Sheu, E. Y., Hammami, A., Marshall, A. G., Eds.; Springer: New York, 2007.
(103) Rosell-Melé, A.; Carter, J. F.; Maxwell, J. R. High-performance liquid chromatography-mass spectrometry of porphyrins by using an atmospheric pressure interface. *J. Am. Soc. Mass Spectrom.* **1996**, *7* (9), 965−971.
(104) Rosell-Mele, A.; Carter, J. F.; Maxwell, J. R. Liquid chromatography/Tandem mass spectrometry of free base alkyl porphyrins for the characterization of the macrocyclic substituents in components of complex mixtures. *Rapid Commun. Mass Spectrom.* **1999**, *13* (7), 568−573.
(105) Chen, X.; Zhang, Y.; Han, J.; Zhang, L.; Zhao, S.; Xu, C.; Shi, Q. Direct nickel petroporphyrin analysis through electrochemical oxidation in electrospray ionization ultrahigh-resolution mass spectrometry. *Energy Fuels* **2021**, *35* (7), 5748−5757.
(106) Purcell, J. M.; Hendrickson, C. L.; Rodgers, R. P.; Marshall, A. G. Atmospheric pressure photoionization Fourier transform ion cyclotron resonance mass spectrometry for complex mixture analysis. *Anal. Chem.* **2006**, *78* (16), 5906−5912.
(107) Purcell, J. M.; Hendrickson, C. L.; Rodgers, R. P.; Marshall, A. G. Atmospheric pressure photoionization proton transfer for complex organic mixtures investigated by Fourier transform ion cyclotron resonance mass spectrometry. *J. Am. Soc. Mass Spectrom.* **2007**, *18* (9), 1682−1689.
(108) Purcell, J. M.; Juyal, P.; Kim, D. G.; Rodgers, R. P.; Hendrickson, C. L.; Marshall, A. G. Sulfur speciation in petroleum: Atmospheric pressure photoionization or chemical derivatization and electrospray ionization Fourier transform ion cyclotron resonance mass spectrometry. *Energy Fuels* **2007**, *21* (5), 2869−2874.
(109) Purcell, J. M.; Rodgers, R. P.; Hendrickson, C. L.; Marshall, A. G. Speciation of nitrogen containing aromatics by atmospheric pressure photoionization or electrospray ionization Fourier transform ion cyclotron resonance mass spectrometry. *J. Am. Soc. Mass Spectrom.* **2007**, *18* (7), 1265−1273.
(110) Purcell, J. M.; Rodgers, R. P.; Hendrickson, C. L.; Marshall, A. G. Atmospheric Pressure Photoionization Proton Transfer for Complex Organic Mixtures Investigated by Fourier Transform Ion Cyclotron Resonance Mass Spectrometry. *J. Am. Soc. Mass Spectrom.* **2007**, *18*, 1682−1689.
(111) Qian, K.; Edwards, K. E.; Siskin, M.; Olmstead, W. N.; Mennito, A. S.; Dechert, G. J.; Hoosain, N. E. Desorption and Ionization of Heavy Petroleum Molecules and Measurement of Molecular Weight Distributions. *Energy Fuels* **2007**, *21* (2), 1042−1047.
(112) McKenna, A. M.; Chacón-Patiño, M. L.; Weisbrod, C. R.; Blakney, G. T.; Rodgers, R. P. Molecular-level characterization of asphaltenes isolated from distillation cuts. *Energy Fuels* **2019**, *33*, 2018.
(113) Chacón-Patiño, M. L.; Nelson, J.; Rogel, E.; Hench, K.; Poirier, L.; Lopez-Linares, F.; Ovalles, C. Vanadium and nickel distributions in Pentane, In-between C5-C7 Asphaltenes, and heptane asphaltenes of heavy crude oils. *Fuel* **2021**, *292*, 120259.
(114) Chacón-Patiño, M. L.; Moulian, R.; Barrère-Mangote, C.; Putman, J. C.; Weisbrod, C. R.; Blakney, G. T.; Bouyssiere, B.; Rodgers, R. P.; Giusti, P. Compositional Trends for Total Vanadium Content and Vanadyl Porphyrins in Gel Permeation Chromatography Fractions Reveal Correlations between Asphaltene Aggregation and Ion Production Efficiency in Atmospheric Pressure Photoionization. *Energy Fuels* **2020**, *34* (12), 16158−16172.
(115) Martinez-Haya, B.; Hortal, A. R.; Hurtado, P.; Lobato, M. D.; Pedrosa, J. M. Laser desorption/ionization determination of

https://doi.org/10.1021/acs.energyfuels.1c02002
Energy Fuels XXXX, XXX, XXX−XXX

molecular weight distributions of polyaromatic carbonaceous compounds and their aggregates. *J. Mass Spectrom.* **2007**, *42*, 701−713.
(116) Cho, Y.; Witt, M.; Jin, J. M.; Kim, Y. K.; Nho, N.-S.; Kim, S. Evaluation of laser desorption ionization coupled to Fourier transform ion cyclotron resonance mass spectrometry to study metalloporphyrin complexes. *Energy Fuels* **2014**, *28* (11), 6699−6706.
(117) Kachadourian, R.; Srinivasan, N.; Haney, C.; Stevens, R. D. An LDI-TOF and ESI mass spectrometry study of a series of β-substituted cationic metalloporphyrins. *J. Porphyrins Phthalocyanines* **2001**, *05*, 507−511.
(118) Xu, H.; Yu, D.; Que, G. Characterization of petroporphyrins in Gudao residue by ultraviolet−visible spectrophotometry and laser desorption ionization-time of flight mass spectrometry. *Fuel* **2005**, *84*, 647−652.
(119) McCarley, T. D.; McCarley, R. L.; Limbach, P. A. Electron-transfer ionization in matrix-assisted laser desorption/ionization mass spectrometry. *Anal. Chem.* **1998**, *70*, 4376−4379.
(120) Ramírez-Pradilla, J. S.; Blanco-Tirado, C.; Combariza, M. Y. Electron-Transfer Ionization of Nanoparticles, Polymers, Porphyrins, and Fullerenes Using Synthetically Tunable α-Cyanophenylenevinylenes as UV MALDI-MS Matrices. *ACS Appl. Mater. Interfaces* **2019**, *11*, 10975−10987.
(121) Giraldo-Dávila, D.; Chacón-Patiño, M. L.; Ramirez-Pradilla, J. S.; Blanco-Tirado, C.; Combariza, M. Y. Selective ionization by electron-transfer MALDI-MS of vanadyl porphyrins from crude oils. *Fuel* **2018**, *226*, 103−111.
(122) Hay, B. P. Methods for molecular mechanics modeling of coordination compounds. *Coord. Chem. Rev.* **1993**, *126* (1−2), 177−236.
(123) Kingsbury, C. J.; Senge, M. O. The shape of porphyrins. *Coord. Chem. Rev.* **2021**, *431*, 213760.
(124) Rio, Y.; Rodríguez-Morgade, M. S.; Torres, T. Modulating the electronic properties of porphyrinoids: A voyage from the violet to the infrared regions of the electromagnetic spectrum. *Org. Biomol. Chem.* **2008**, *6* (11), 1877−1894.
(125) De Visser, S. P.; Stillman, M. J. Challenging density functional theory calculatins wth hemes and porphyrins. *Int. J. Mol. Sci.* **2016**, *17* (4), 519.
(126) Kaplan, W. A.; Suslick, K. S.; Scott, R. A. Core Size and Flexibility of Metallohydroporphyrin Macrocycles. Implications for F430 Coordination Chemistry. *J. Am. Chem. Soc.* **1991**, *113* (26), 9824−9827.
(127) Munro, O. Q.; Bradley, J. C.; Hancock, R. D.; Marques, H. M.; Marsicano, F.; Wade, P. W. Molecular mechanics study of the ruffling of metalloporphyrins. *J. Am. Chem. Soc.* **1992**, *114*, 7218−7230.
(128) Marques, H. M.; Munro, O. Q.; Grimmer, N. E.; Levendis, D. C.; Marsicano, F.; Pattrick, G.; Markoulides, T. A Force Field for Molecular Mechanics Studies of Iron Porphyrins. *J. Chem. Soc., Faraday Trans.* **1995**, *91* (12), 1741−1749.
(129) Munoz, G.; Gunessee, B. K.; Begue, D.; Bouyssiere, B.; Baraille, I.; Vallverdu, G.; Santos Silva, H. Redox activity of nickel and vanadium porphyrins: A possible mechanism behind petroleum genesis and maturation? *RSC Adv.* **2019**, *9* (17), 9509−9516.
(130) Kadiev, K. M.; Gyul'maliev, A. M.; Khadzhiev, S. N. Quantum-Chemical Modeling of Strength of Organometallic Bonds in Oil. *Pet. Chem.* **2015**, *55* (8), 609−617.
(131) Song, X.-Z.; Jaquinod, L.; Jentzen, W.; Nurco, D. J.; Jia, S.-L.; Khoury, R. G.; Ma, J.-G.; Medforth, C. J.; Smith, K. M.; Shelnutt, J. A. Metal dependence of the contributions of low-frequency normal coordinates to the sterically induced distortions of meso-dialkyl-substituted porphyrins. *Inorg. Chem.* **1998**, *37* (8), 2009−2019.
(132) Skopec, C. E.; Robinson, J. M.; Cukrowski, I.; Marques, H. M. Using Artificial Neural Networks to Develop Molecular Mechanics Parameters for the Modelling of Metalloporphyrins. III. Five Coordinate Zn(II) Porphyrins and the Metalloprophyrins of the Early 3d Metals. *J. Mol. Struct.* **2005**, *738* (1), 67−78.
(133) Marques, H. M.; Brown, K. L. Molecular mechanics and molecular dynamics simulations of porphyrins, metalloporphyrins, heme proteins and cobalt corrinoids. *Coord. Chem. Rev.* **2002**, *225* (1), 123−158.
(134) Cundari, T. R.; Saunders, L.; Sisterhen, L. L. Molecular modeling of vanadium-oxo complexes. A comparison of quantum and classical methods. *J. Phys. Chem. A* **1998**, *102* (6), 997−1004.
(135) Stoll, L. K.; Zgierski, M. Z.; Kozlowski, P. M. Density Functional Theory Analysis of Nickel Octaethylporphyrin Ruffling. *J. Phys. Chem. A* **2002**, *106* (1), 170−175.
(136) Czader, A.; Czernuszewicz, R. S. Fingerprinting petroporphyrin structures with vibrational spectroscopy. Part 7. Calculations using density functional theory of the molecular structures and structure-sensitive vibrational modes of type II nickel(II) cycloalkanoporphyrins. *Org. Geochem.* **2007**, *38*, 250−266.
(137) Stoyanov, S. R.; Yin, C.-X.; Gray, M. R.; Stryker, J. M.; Gusarov, S.; Kovalenko, A. Density functional theory investigation of the fffect of axial coordination and annelation on the absorption spectroscopy of nickel(II) and vanadyl porphyrins relevant to bitumen and crude oils. *Can. J. Chem.* **2013**, *91* (9), 872−878.
(138) Santos Silva, H.; Sodero, A. C. R.; Korb, J.-P.; Alfarra, A.; Giusti, P.; Vallverdu, G.; Bégué, D.; Baraille, I.; Bouyssiere, B. The role of metallporphyrins on the physical-chemical properties of petroleum fluids. *Fuel* **2017**, *188*, 374−381.
(139) Mousavi, M.; Hosseinnezhad, S.; Hung, A. M.; Fini, E. H. Preferential adsorption of nckel porphyrin to resin to increase asphaltene precipitation. *Fuel* **2019**, *236*, 468−479.
(140) Mousavi, M.; Fini, E. H. Non-covalent π-stacking interactions between asphaltene and porphyrins on surfaces and nanostructures with periodic DFT calculations. *J. Chem. Inf. Model.* **2020**, *60* (10), 4856−4866.
(141) da Costa, L. M.; Stoyanov, S. R.; Gusarov, S.; Tan, X.; Gray, M. R.; Stryker, J. M.; Tykwinski, R.; de M. Carneiro, J. W.; Seidl, P. R.; Kovalenko, A. Density Functional Theory investigation of the contributions of pi = pi stacking and hydrogen-bonding interactions to the aggregation of model asphaltene compounds. *Energy Fuels* **2012**, *26* (5), 2727−2735.
(142) Santos Silva, H.; Alfarra, A.; Vallverdu, G.; Begue, D.; Bouyssiere, B.; Baraille, I. Impact of H-Bonds and Porphyrins on Asphaltene Aggregation As Revealed by Molecular Dynamics Simulations. *Energy Fuels* **2018**, *32* (11), 11153−11164.
(143) Santos Silva, H.; Alfarra, A.; Vallverdu, G.; Begue, D.; Bouyssiere, B.; Baraille, I. Role of the porphyrins and demulsifiers in the aggregation process of asphaltenes at water/oil interfaces under desalting conditions: A molecular dynamics study. *Pet. Sci.* **2020**, *17*, 797−810.
(144) Gruden-Pavlović, M.; Grubišić, S.; Zlatar, M.; Niketić, S. R. Molecular mechanics study of nickel(II)octaethylporphyrin adbsored on graphite(0001). *Int. J. Mol. Sci.* **2007**, *8* (8), 810−829.
(145) Zaragoza, I. P.; Santamaria, R.; Salcedo, R. The interaction of vanadyl porphyrin with the HY Zeolite surface. *J. Mol. Catal. A: Chem.* **2009**, *307* (1), 64−70.
(146) Torres, A.; Amaya Suárez, J.; Remesal, E.; Márquez, A. M.; Fernández Sanz, J.; Rincón Cañibano, C. Adsorption of prototypical asphaltenes on silica: First-principles DFT simulations including dispersion corrections. *J. Phys. Chem. B* **2018**, *122* (2), 618−624.
(147) Chilukuri, B.; Mazur, U.; Hipps, K. W. Structure, properties, and reactivity of porphyrins on surfaces and nanostructures with periodic DFT calculations. *Appl. Sci.* **2020**, *10* (3), 740.
(148) Myradalyyev, S.; Limpanuparb, T.; Wang, X.; Hirao, H. Comparative Computational Analysis of Binding Energies Between Several Divalent First-Row Transition Metals (Cr2+, Mn2+, Fe2+, Co2+, Ni2+, and Cu2+) and Ligands (porphine, Corrin, and TMC). *Polyhedron* **2013**, *52*, 96−101.
(149) Ju, L.; Liu, T.; Lu, J.; Zhou, Y.; Wei, Q.; Li, S.; Ding, S.; Zhang, Y.; Shi, Q. Transformation of nickel octaethylporphrine in hydrodemetallization reactions. *Energy Fuels* **2016**, *30* (9), 6933−6941.

https://doi.org/10.1021/acs.energyfuels.1c02002
Energy Fuels XXXX, XXX, XXX−XXX

(150) Li, Y.; Shang, H.; Zhang, Q.; Elabyouki, M.; Zhang, W. Theoretical study of the structure and properties of Ni/V porphyrins under microwave electric field: A DFT study. *Fuel* **2020**, *278*, 118305.
(151) García-Cruz, I.; Martínez-Magadán, J. M.; Alvarez-Ramirez, F.; Salcedo, R.; Illas, F. Theoretical study of nickel porphyrinate derivatives related to catalyst dopant in the oil industry. *J. Mol. Catal. A: Chem.* **2005**, *228* (1), 195−202.
(152) Salcedo, R.; Martínez, L. M. R.; Martínez-Magadán, J. M. Theoretical study of high-valent vanadium oxo-porphyrins as a dopant of crude oil. *J. Mol. Struct.: THEOCHEM* **2001**, *542* (1), 115−121.
(153) Soret, J.-L. Analyse spectrale: Sur le specre d'absorption du sang dans la partie violette et ultra-violette. *Comptes rendu de l'Academie des sciences* **1883**, *97*, 1269−1273.
(154) Speight, J. G. *The Desulfurization of Heavy Oils and Residua*, 2nd ed.; Marcel Dekker, Inc.: New York, 2000; Vol. *78*.
(155) Speight, J. *Handbook of Petroleum Analysis*; John Wiley & Sons, 2001; pp 232−233.
(156) Speight, J. G. *Handbook of Petroleum Product Analysis*; John Wiley & Sons, 2015.
(157) Wei, W.; Bennett, C. A.; Tanaka, R.; Hou, G.; Klein, M. T. Detailed kinetic models for catalytic reforming. *Fuel Process. Technol.* **2008**, *89* (4), 344−349.
(158) Zheng, F. *Molecular Composition and Structure of Metal Compounds in Asphaltene*; China University of Petroleum Beijing: Beijing, 2021.
(159) Bai, P.; Etim, U. J.; Yan, Z.; Mintova, S.; Zhang, Z. G.; Zhong, Z.; Gao, X. Fluid catalytic cracking technology: current status and recent discoveries on catalyst contamination. *Catal. Rev.: Sci. Eng.* **2019**, *61* (3), 333−405.
(160) Vogt, E. T. C.; Weckhuysen, B. M. Fluid catalytic cracking: recent developments on the grand old lady of zeolite catalysis. *Chem. Soc. Rev.* **2015**, *44* (20), 7342−7370.
(161) YangDong, X.; YuanBin, Y.; Ying, Z.; Huang, K. Q. Tackling high nickel feedstock. *Hydrocarb. Eng.* **2020**, *25* (11), 19−22.
(162) Liu, T. *Transformation of Metal Compounds in the Vacuum Residuum Hydrodemetallization and Design of HDM Catalysts*; China University of Petroleum Beijing: Beijing, 2016.
(163) Ali, M. F.; Abbas, S. A review of methods for the demetallatization of residual fuel oils. *Fuel Process. Technol.* **2006**, *87* (7), 573−584.
(164) Rodríguez, E.; Félix, G.; Ancheyta, J.; Trejo, F. Modeling of hydrotreating catalyst deactivation for heavy oil hydrocarbons. *Fuel* **2018**, *225*, 118−133.
(165) Sullivan, R. F.; Boduszynski, M. M.; Fetzer, J. C. Molecular-transformations in hydrotreating and hydrocracking. *Energy Fuels* **1989**, *3* (5), 603−612.
(166) Topsoe, H.; Bjerne, C. S.; Massoth, F. E. *Hydrotreating Catalysis: Science and Technology*; Springer-Verlag: New York, 1996; Vol. *11*, pp 1−310.
(167) Wiwel, P.; Knudsen, K.; Zeuthen, P.; Whitehurst, D. Assessing compositional changes of nitroge compounds during hydrotreating of typical diesel range gas oils using a novel preconcentration technique coupled with gas chromatography and atomic emission detection. *Ind. Eng. Chem. Res.* **2000**, *39* (2), 533−540.
(168) Fish, R. H.; Komlenic, J. J.; Wines, B. K. Characterization and comparison of vanadyl and nickel compounds in heavy crude petroleums and asphaltenes by reverse-phase and size-excluded liquid chromatography/graphite furnace atomic absorption spectrometry. *Anal. Chem.* **1984**, *56*, 2452−2460.
(169) Yen, T. F. *The Role of Trace Metals in Petroleum*; Ann Arbor Science: Ann Arbor, MI, 1975.
(170) Dickson, F. E.; Kunesh, C. J.; McGinnis, E. L.; Petrakis, L. Use of electron spin resonance to characterize the vanadium(IV)-sulfur species in petroleum. *Anal. Chem.* **1972**, *44* (6), 978−981.
(171) Dickie, J. P.; Yen, T. F. Macrostructures of the asphaltic fractions by various instrumental methods. *Anal. Chem.* **1967**, *39* (14), 1847−1852.
(172) Tynan, E. C.; Yen, T. F. Association of vanadium chelates in petroleum asphaltenes as studied by E.S.R. *Fuel* **1969**, *48* (2), 191−208.
(173) Yen, T. F.; Boucher, W.; Dickie, J. P.; Tynan, E. C.; Vaughan, G. B. Vanadium Complexes and Porphyrins in Asphaltenes. *J. Inst. Petrol.* **1969**, *55*, 87.
(174) Wu, Y.; Zheng, F.; Lu, J.; Shi, Q. Characterization of parts of vanadyl non-porphyrins in petroleum. *Acta Petrolei Sinica (Petroleum Processing Section)* **2020**, *36* (5), 1003−1010.
(175) Moulian, R.; Zheng, F.; Salvato Vallverdu, G.; Barrere-Mangote, C.; Shi, Q.; Giusti, P.; Bouyssiere, B. Understanding the vanadium-asphaltene nanoaggregate link with silver triflate complexation and GPC ICP-MS analysis. *Energy Fuels* **2020**, *34* (11), 13759−13766.
(176) Zheng, F.; Zhang, Y.; Zhang, Y.; Han, Y.; Zhang, L.; Bouyssiere, B.; Shi, Q. Aggregation of petroporphyrins and fragmentation of porphyrin ions: Characterized by TIMS-TOF MS and FT-ICR MS. *Fuel* **2021**, *289*, 119889.
(177) Wu, Y. *Molecular Composition of Petroleum Non-Porphyrin*; China University of Petroleum Beijing: Beijing, 2017.
(178) Charrie-Duhaut, A.; LEmoine, S.; Adam, P.; Connan, J.; Albrecht, P. Abiotic oxidation of petroleum bitumens under natural conditions. *Org. Geochem.* **2000**, *31* (10), 977−1003.
(179) Ocampo, R.; Riva, A.; Trendel, J. M.; Riolo, J.; Callot, H. J.; Albrecht, P. Petroporphyrins as biomarkers in oil-oil and oil-source rock correlations. *Energy Fuels* **1993**, *7* (2), 191−193.
(180) Blumer, M. Separation of porphyrins by paper chromatography. *Anal. Chem.* **1956**, *28* (11), 1640−1644.
(181) Barwise, A. J. G. Role of nickel and vanadium in petroleum classification. *Energy Fuels* **1990**, *4* (6), 647−652.
(182) Szymczak-Zyla, M.; Kowalewska, G.; Louda, J. W. Chlorophyll-*a* and derivatives in recent sediments as indicators of productivity and depositional conditions. *Mar. Chem.* **2011**, *125*, 39−48.
(183) Kashiyama, Y.; Ogawa, N. O.; Shiro, M.; Tada, R.; Kitazato, H.; Ohkouchi, N. Reconstruction of the biogeochemistry and ecology of photoautotrophs based on the nitrogen and carbon isotopic compositions of vanadyl porphyrins from Miocene siliceous sediments. *Biogeosciences Discuss.* **2008**, *5*, 361−409.
(184) Keely, B. J.; Prowse, W. G.; Maxwell, J. R. The Treibs hypothesis: An evaluation based on structural studies. *Energy Fuels* **1990**, *4* (6), 628−634.
(185) Fookes, C. J. R. Structure determination of nickel(II) deoxophylloerythroetioporphyrin and a C30 homologue from an oil shale: Evidence that petroporphyrins are derived from chlorophyll. *J. Chem. Soc., Chem. Commun.* **1983**, 1472−1473.
(186) Gibbison, R.; Peakman, T. M.; Maxwell, J. R. Novel porphyrins as molecular fossils for anoxygenic photosynthesis. *Tetrahedron Lett.* **1995**, *36*, 9057−9060.
(187) Kashiyama, Y.; Shiro, M.; Tada, R.; Ohkouchi, N. A novel vanadyl alkylporphyrins from geological samples: a possible derivative of divinylchlorophylls or bacteriochlorophyll a. *Chem. Lett.* **2007**, *36*, 706−707.
(188) Kashiyama, Y.; Ogawa, N. O.; Kuroda, J.; Shiro, M.; Nomoto, S.; Tada, R.; Kitazato, H.; Ohkouchi, N. Diazotrophic cyanobacteria as the major photoautotrophs during mid- Cretaceous oceanic anoxic events: nitrogen and carbon isotopic evidence from sedimentary porphyrin. *Org. Geochem.* **2008**, *39* (5), 532−549.
(189) Keely, B.J.; Harris, P.G.; Popp, B.N.; Hayes, J.M.; Meischner, D.; Maxwell, J.R. Porphyrin and chlorin distributions in a Lake Pliocene lacustrine sediment. *Geochim. Cosmochim. Acta* **1994**, *58*, 3691−3701.
(190) Boreham, C. J.; Fookes, C. J. R.; Popp, B. N.; Hayes, J. M. Origins of etioporphyrins in sediments: evidence from stable carbon isotopes. *Geochim. Cosmochim. Acta* **1989**, *53*, 2451−2455.
(191) Boreham, C. J.; Fookes, C. J. R.; Popp, B. N.; Hayes, J. M. Origin of petroporphyrins. 2. Evidence from stable isotopes. *Energy Fuels* **1990**, *4*, 658−661.

https://doi.org/10.1021/acs.energyfuels.1c02002
Energy Fuels XXXX, XXX, XXX−XXX

(192) Chicarelli, M. I.; Hayes, J. M.; Popp, B. N.; Eckardt, C. B.; Maxwell, J. R. Carbon and nitrogen isotopic compositions of alkyl porphyrins from the Triassic Serpiano oil shale. *Geochim. Cosmochim. Acta* **1993**, *57*, 1307−1311.
(193) Kashiyama, Y.; Kitazato, H.; Ohkouchi, N. An improved method for isolation and purification of sedimentary porphyrins by high-performance liquid chromatography for compound specific isotopic analysis. *J. Chromatogr. A* **2007**, *1138*, 73−83.
(194) Boggess, J. M.; Czernuszewicz, R. S.; Lash, T. D. Fingerprinting petroporphyrin structures with vibrational spectroscopy. Part 6. resonance Raman characterization of regioisomets of nickel(II) benzoetioporphyrin. *Org. Geochem.* **2002**, *33*, 1111−1126.
(195) Gueneli, N.; McKenna, A. M.; Ohkouchi, N.; Boreham, C. J.; Beghin, J.; Javaux, E. J.; Brocks, J. J. 1.1-Billion-Year-Old Porphyrins Establish a Marine Ecosystem Dominated by Bacterial Primary Producers. *Proc. Natl. Acad. Sci. U. S. A.* **2018**, *115* (30), E6978−E6986.
(196) Grosjean, E.; Adam, P.; Connan, J.; Albrecht, P. Effects of weathering on nickel and vanadyl porphyrins of a Lower Toarcian shale of the Paris basin. *Geochim. Cosmochim. Acta* **2004**, *68* (4), 789.
(197) Zheng, F.; Zhu, G.-Y.; Chen, Z.-Q.; Zhao, Q.-L.; Shi, Q. Molecular composition of vanadyl porphyrins in the gilsonite. *J. Fuel Chem. Technol.* **2020**, *48* (5), 562−567.

NOTE ADDED AFTER ASAP PUBLICATION

This paper was published ASAP on August 19, 2021, with an incorrect reference citation in Figure 3 caption. The corrected version was reposted on August 23, 2021.

https://doi.org/10.1021/acs.energyfuels.1c02002
Energy Fuels XXXX, XXX, XXX−XXX